



HAL
open science

Toxicity of binary mixtures of pesticides to the marine microalgae *Tisochrysis lutea* and *Skeletonema marinoi*: Substance interactions and physiological impacts

Valentin Dupraz, Dominique Menard, Farida Akcha, H  l  ne Budzinski, Sabine Stachowski-Haberhorn

► To cite this version:

Valentin Dupraz, Dominique Menard, Farida Akcha, H  l  ne Budzinski, Sabine Stachowski-Haberhorn. Toxicity of binary mixtures of pesticides to the marine microalgae *Tisochrysis lutea* and *Skeletonema marinoi*: Substance interactions and physiological impacts. *Aquatic Toxicology*, 2019, 211, pp.148-162. 10.1016/j.aquatox.2019.03.015 . hal-02339522

HAL Id: hal-02339522

<https://hal.science/hal-02339522>

Submitted on 22 Oct 2021

HAL is a multi-disciplinary open access archive for the deposit and dissemination of scientific research documents, whether they are published or not. The documents may come from teaching and research institutions in France or abroad, or from public or private research centers.

L'archive ouverte pluridisciplinaire **HAL**, est destin  e au d  p  t et    la diffusion de documents scientifiques de niveau recherche, publi  s ou non,   manant des   tablissements d'enseignement et de recherche fran  ais ou   trangers, des laboratoires publics ou priv  s.



Distributed under a Creative Commons Attribution - NonCommercial 4.0 International License

Toxicity of binary mixtures of pesticides to the marine microalgae *Tisochrysis lutea* and *Skeletonema marinoi*: substance interactions and physiological impacts

Valentin Dupraz^{1,2}, Dominique Ménard¹, Farida Akcha¹, H el ene Budzinski^{3,4}, Sabine Stachowski-Haberkorn¹

¹ Ifremer, Laboratoire d' cotoxicologie, rue de l' le d'Yeu, BP 21105, F-44311 Nantes cedex 03, France

² Universit  de Nantes, UFR Sciences et Techniques, 2, rue de la Houssini re, BP 92208, 44322 Nantes Cedex 03, France

³ Universit  de Bordeaux, UMR 5805, EPOC, Laboratoire de Physico Toxico Chimie de l'environnement, 351 Cours de la Lib ration, CS 10004, F-33405 Talence Cedex, France

⁴ CNRS, UMR 5805, EPOC, Laboratoire de Physico Toxico Chimie de l'environnement, 351 Cours de la Lib ration, CS 10004, F-33405 Talence Cedex, France

* Corresponding author. E-mail address: valentin.dupraz@ifremer.fr

Highlights

- The toxicity of binary pesticide mixtures was evaluated on two microalgal species.
- Effects of three selected mixtures were then examined on five physiological functions.
- Effects on microalgal physiology were linked to the pesticide's toxic mode of action.
- Mixed isotroturon and metazachlor had significant synergistic effects on *S. marinoi*.
- Observed synergy could be due to a combined effect on the photosynthetic apparatus.

Abstract

This study screened binary mixtures of pesticides for potential synergistic interaction effects on growth of the marine microalgae *Tisochrysis lutea* and *Skeletonema marinoi*. It also examined the single and combined effects of three of the most toxic substances on microalgal physiology.

Single substances were first tested on each microalgal species to determine their respective EC₅₀ and concentration-response relationships. The toxicity of six and seven binary mixtures was then evaluated in microplate experiments on the growth of *T. lutea* and *S. marinoi*, respectively, using two mixture modelling approaches: isobolograms and the MIXTOX tool, based on Concentration Addition (CA) or Independent

Action (IA) models. Significant cases of antagonism (for both species) and synergism (for *S. marinoi*) were observed for the mixtures of isoproturon and spiroxamine, and isoproturon and metazachlor, respectively.

These two mixtures, together with that of isoproturon and diuron, for which additivity was observed, were further studied for their impacts on the physiology of each species. Exposures were thus made in culture flasks at three concentrations, or concentration combinations for mixtures, selected to cause 25%, 50% and 75% growth rate inhibition. The effects of the selected pesticides singly and in combination were evaluated at three perceived effect concentrations on esterase metabolic activity, relative lipid content, cytoplasmic membrane potential and reactive oxygen species (ROS) content by flow cytometry, and on photosynthetic quantum yield (ϕ'_M) by PAM-fluorescence.

Isoproturon and diuron singly and in mixtures induced 20–40% decreases in ϕ'_M which was in turn responsible for a significant decrease in relative lipid content for both species. Spiroxamine and metazachlor were individually responsible for an increase in relative lipid content (up to nearly 300% for metazachlor on *S. marinoi*), as well as cell depolarization and increased ROS content. The mixture of isoproturon and metazachlor tested on *S. marinoi* caused a 28–34% decrease in ϕ'_M that was significantly higher than levels induced by each of substances when tested alone. This strong decrease in ϕ'_M could be due to a combined effect of these substances on the photosynthetic apparatus, which is likely the cause of the synergy found for this mixture.

Keywords

ROS; photosynthesis; lipids; synergy; isoproturon; metazachlor

1. Introduction

A significant amount of the pesticides used in agriculture is lost during and after their application due to dispersion processes such as spray-drift, leaching and runoff (Wauchope et al., 2003; Ravier et al., 2005; Southwick et al., 2009; Larsbo et al., 2016; Zhang et al., 2018). Thus, numerous pesticides can be detected in environments ranging from freshwater ecosystems near agricultural fields to estuarine and coastal waters (Caquet et al., 2013; Moschet et al., 2014; Cruzeiro et al., 2015). Pesticides can be grouped in many different classes according to their usage (herbicides, insecticides, fungicides, rodenticides, algacides *etc.*) and include general biocides (not always permitted in agriculture) and phytosanitary products (PPs). These substances possess various modes of action (MOA) that may potentially harm organisms besides their initial targets, known as non-target organisms.

Microalgae are among the non-target aquatic organisms exposed to pesticides. Indeed, many herbicides target physiological structures (*e.g.*, photosystems) that are the same between microalgae and targeted plants and may therefore have a significant impact. As primary producers, microalgae constitute the basis of aquatic ecological networks, so it is important to study the ways they are impacted by pesticides (Hlaili et al., 2014).

Their photosynthesis is responsible for nearly 50% of oxygen production and carbon dioxide fixation on earth (Chapman, 2013; Beardall and Raven, 2016). In addition to their ecological relevance, the relatively short generation time of microalgae and their ease of culture in the laboratory have led to the development of several standard toxicity assays using different species. These assays include both freshwater (ISO 8692:2012, 2012) and marine (ISO 10253:2016, 2016) species and allow the establishment of standard ecotoxicological values, such as EC₅₀ (effective concentration inducing a 50% effect on a selected endpoint) or NOEC (no-observed effect concentration).

In most contaminated aquatic environments, chemicals are present as mixtures (González-Pleiter et al., 2013; Magdaleno et al., 2015). Even though the toxicity of environmental mixtures is generally driven by only a few compounds (de Zwart and Posthuma, 2005; Belden et al., 2007; Vallotton and Price, 2016; Holmes et al., 2018), testing the toxicity of single substances might not be sufficient as interactions between substances can occur. In the review by Cedergreen (2014), it was shown that 26% and 7% of the investigated binary mixtures of antifouling biocides and pesticides, respectively, were synergistic, *i.e.*, the toxicity induced by the mixture was at least double the predicted level. Due to the potentially higher toxicity of mixtures, several studies have evaluated the interactive effects resulting from binary mixtures of various chemicals (Altenburger et al., 1990; Cedergreen et al., 2006, 2007, 2013; Koutsaftis and Aoyama, 2006; Sørensen et al., 2007; Bao et al., 2008). In these studies, the Concentration Addition (CA, Loewe and Muischnek, 1926) and/or Independent Action (IA, Bliss, 1939) models were used as references to predict the toxicity resulting from the joint action of chemicals in binary mixtures. The resulting interaction effect of such mixtures was then defined by comparing experimental and predicted (*i.e.*, by the CA or IA model) toxicity responses.

In ecotoxicological studies, growth endpoints such as biomass, growth rate (Vendrell et al., 2009; Bergtold and Dohmen, 2011; Pérez et al., 2011; Nagai and De Schamphelaere, 2016) or photosystem II (PSII) quantum yield (Magnusson et al., 2008; Sjollem et al., 2014) are often used to evaluate effects on microalgae. These endpoints measured by using time- and cost-effective short-term assays allow the toxicity of single substances or mixtures to be assessed and have proven very useful for identifying which substances are the most toxic.

A promising tool for examining the underlying causes of toxicity to microalgal growth is flow cytometry. In addition to cell density measurements, flow cytometry can be used to analyse several morphological parameters, such as relative cell size and complexity and relative fluorescence, which is related to pigment content (Marie et al., 2005; Stachowski-Haberkorn et al., 2013; Mansano et al., 2017). Using fluorescent dyes specific to particular physiological functions, several studies have shown the usefulness of flow cytometry to indicate the toxicity of certain chemicals to microalgae (Prado et al., 2009, 2012; Rioboo et al., 2011; Stachowski-Haberkorn et al., 2013; Seoane et al., 2014, 2017; Esperanza et al., 2015; Dupraz et al., 2016; González-Pleiter et al., 2017). The most commonly investigated physiological functions in these studies are viability, general metabolic activity (often measured by non-specific esterase activity) and reactive oxygen species (ROS), whose accumulation following exposure to certain contaminants can cause oxidative stress and thus cell damage. Effects of pollutants on cytoplasmic membrane potential, relative lipid content and

DNA damage have been examined less often. Investigating the effects of chemical substances on such physiological functions can improve our understanding of their toxic MOA.

In this study, seven pesticides, including the biocides isoproturon and diuron and the PPs metazachlor, chlorpyrifos-methyl, azoxystrobin, quinoxifen and spiroxamine, were selected and their effects on the growth and physiology of the marine microalgae *Tisochrysis lutea* and *Skeletonema marinoi* were investigated. Isoproturon and diuron are two PSII inhibitors previously used as herbicides in agriculture and, in the case of diuron, as an antifouling biocide. Today their use is only permitted as films or construction material preservatives (European Chemicals Agency, 2018). Their high toxicity towards microalgae has been reported in numerous studies (Arzul et al., 2006; Bao et al., 2011; Stachowski-Haberkorn et al., 2013; Sjollem et al., 2014; Dupraz et al., 2016, 2018). Metazachlor is a herbicide belonging to the chloroacetamide family that inhibits the synthesis of very long chain fatty acids (VLCFAs) thus disturbing cell division (Götz and Böger, 2004; Vallotton et al., 2008). Its toxicity towards microalgae has only rarely been examined in the literature (Junghans et al., 2003), although another chloroacetamide, S-metolachlor, has received more attention (Debenest et al., 2009; Ebenezer and Ki, 2013; Thakkar et al., 2013; Coquillé et al., 2018). The toxicity of the other PPs to microalgae has rarely been explored, although one study reported the effect of azoxystrobin on a freshwater alga (Ochoa-Acuña et al., 2009). Consequently, their toxic MOAs towards microalgae are not well known. Regarding the environmental concentrations of these substances, diuron and isoproturon were found at maximum concentrations of 0.27 and 0.19 $\mu\text{g L}^{-1}$ in the Vilaine estuary (France) (Caquet et al., 2013). Metazachlor was found in both surface and ground water at concentrations ranging from 0.1 to 100 $\mu\text{g L}^{-1}$ (Mohr et al., 2007, 2008), while chlorpyrifos-methyl was found at a maximum concentration of 0.052 $\mu\text{g L}^{-1}$ in the surface waters of river Aspropotamos (Greece) (Papadakis et al., 2015). Finally, the fungicide azoxystrobin was detected at an average concentration of 2.15 $\mu\text{g L}^{-1}$ in the surface waters of the Rio Formosa lagoon (Portugal) during spring (Cruzeiro et al., 2015). No information regarding the environmental concentrations of quinoxifen and spiroxamine in surface waters was found in the current literature.

To identify potential synergistic interactions, this study aimed first to evaluate the single and combined effects of those pesticides as binary mixtures on the growth of two marine microalgae. In a second step, the toxicity of three out of the eight tested binary mixtures, selected on the basis of their combined effect: additive, synergistic or antagonistic, was investigated at a deeper level. The effects of the single substances and their combinations on the physiology of the two microalgal species were explored to improve our comprehension of the toxic MOA of the interaction resulting from their mixture. To this end, effects on growth, PSII quantum yield and four additional physiological endpoints were examined by flow cytometry: esterase activity, relative lipid content, cytoplasmic membrane potential, and ROS content.

2. Materials and methods

2.1. Chemical / toxicant preparation

All chemicals tested in this study (Table 1) were purchased from Sigma-Aldrich (PESTANAL[®], analytical standard). Stock solutions were prepared in pure methanol ($\geq 99\%$), except for diuron and spiroxamine, which were prepared in pure DMSO ($\geq 99\%$) and acetone ($\geq 99\%$), respectively. These stock solutions were diluted in their respective solvents to make working solutions. All solutions were quantified by liquid or gas chromatography tandem mass spectrometry (LC-MS/MS or GC-MS/MS). The chemical analysis method used for quantification and the concentrations measured are available in the supplementary material (Table S1). In all toxicity tests, the nominal concentrations were calculated using the measured concentrations of the stock solutions.

2.2. Microalgal cultures

The marine microalga *Tisochrysis lutea* (*T. lutea*) CCAP 927/14 was purchased from the Culture Center of Algae and Protozoa (CCAP, Oban, Scotland). The marine diatom *Skeletonema marinoi* (*S. marinoi*) AC174 was purchased from the University of Caen Algalbank (Caen, France). Microalgal cultures were maintained in sterile f/2 (*T. lutea*) and f/2-silica (*S. marinoi*) media (Guillard and Ryther, 1962; Guillard, 1975; Table S2) at $20 \pm 1^\circ\text{C}$, in a thermostatic chamber at $130 \mu\text{mol m}^{-2} \text{s}^{-1}$ (Quantometer Li-Cor Li-250 equipped with a spherical sensor), with a dark:light cycle of 8:16 h. Cultures were grown in 100 mL round borosilicate sterile glass flasks previously heated to 450°C for 6 h, autoclaved for 20 min at 121°C and then filled with 50 mL of sterile culture medium. Cultures were diluted weekly to maintain an exponential growth phase.

2.3. Exposure experiments

2.3.1. Binary mixtures in microplates

Prior to the binary mixture experiments, concentration-response experiments were performed for each chemical and microalgal species to determine their $\text{EC}_{50\text{s}}$, *i.e.*, the concentration inducing a 50% inhibition of the growth rate calculated after a 96-h exposure (Table 1; supplementary material: Table S3, Figure S1, S3 and S4).

Binary mixtures were then made to evaluate the interaction effects of selected pesticide mixtures on algae growth, using the concentration-response surface approach (Gessner, 1995; White et al., 2004). The detailed procedure is described in Dupraz et al. (2018), and additional information is given as supplementary material (Table S4 and Figure S4). Briefly, toxicity assays were run for 96 h in sterile 48-well transparent polystyrene microplates (Greiner Bio-One GmbH, cat. 677102, untreated), each well being filled with 0.90 mL of sterile f/2 or f/2-Si culture medium and 0.10 mL of microalgal culture. For each binary mixture, the two single chemicals (considered as mixture ratios of 100:0% and 0:100%) and their mixtures at perceived

effective concentration ratios of 75:25%, 50:50% and 25:75% were tested using six concentrations in triplicate. The initial cell density was 2.00×10^4 cell mL⁻¹ at the beginning of exposure and the final volume of each well was 1.00 mL.

Among the 36 possible binary combinations, eight were selected based on the toxicity of the chemicals singly, their expected MOA, and whether or not tests on such mixtures had been reported in the literature. The five following binary mixtures were tested on both species: ISO¹+DIU; ISO+AZO; ISO+QUI; ISO+SPI; SPI+QUI. Additionally, a SPI+CHL-M mixture was tested on *T. lutea* only, as CHL-M did not induce any effect in *S. marinoi* in the range of tested concentrations. Similarly, mixtures of ISO+MET and SPI+MET were only tested on *S. marinoi* as MET did not affect *T. lutea* (Table 1).

2.3.2. Binary mixtures in culture flasks

Based on the results obtained during the microplate experiments, three binary mixtures likely to induce three different types of interactive effect (additivity, antagonism and synergy) were then selected to be tested in 96-h culture flask toxicity assays. These experiments were designed to evaluate the interaction effects of the selected mixtures on several physiological functions by flow cytometry and PAM-fluorescence, thus requiring more microalgal material.

As described in §2.2, 100 mL round borosilicate sterile glass flasks were used for the assays and filled with 49.0 mL of sterile f/2 or f/2-Si culture medium. For each binary mixture, the two single chemicals and their 50:50% mixture ratio were tested at three concentrations in triplicate accompanied by three solvent controls containing the highest solvent percentage used in the assay (supplementary material: Table S5). Chemicals and solvents were spiked directly into the culture flasks. The three exposure concentrations were calculated to induce specific inhibition effects of 25%, 50% and 75% using the previously determined concentration-response relationships for the single chemicals. For mixtures, concentrations of each substance were calculated based on their individual EC₅₀s, so that the sum of Toxic Units (TU) of the 50:50% mixture ratio ($\Sigma TU_{50:50}$; see §2.4.2.1 for further details) was equal to 0.5, 1 and 1.5 TU respectively. For each species, after measurement of the cell density by flow cytometry, the microalgal culture was diluted into an intermediate culture at 1.00×10^6 cell mL⁻¹. Then, 1.00 mL of the intermediate culture was added to each culture flask to give a concentration of 2.00×10^4 cell mL⁻¹ at the beginning of exposure. The final volume in each culture flask was 50.0 mL.

Flasks were sampled (0.50 mL) every 24 h, during the light phase to evaluate microalgal growth using cell density measured by flow cytometry, as described below in §2.5. On the last day of exposure, an additional 2.00 mL were sampled for PSII effective quantum yield (ϕ'_M , §2.5.2) measurement; 5×0.50 mL were sampled for subsequent analyses of the selected physiological endpoints using fluorescent dyes.

¹ Abbreviations: ISO = isoproturon; DIU = diuron; AZO = azoxystrobin; QUI = quinoxifen; SPI = spiroxamine; CHL-M = chlorpyrifos-methyl; MET = metazachlor.

2.4. Statistical analysis

2.4.1. Concentration-response

Concentration-response analyses were carried out using R software 3.5.1 with the *drc* package (Ritz and Streibig, 2005; Ritz et al., 2015). Each chemical was tested using six concentrations in triplicate and a single three-parameter log-logistic regression model (LL.3) was applied (Equation 1),

$$U = \frac{d}{\left(1 + \left(\frac{x}{EC_{50}}\right)^b\right)} \quad (1)$$

where U is the response, in our case the 96-h growth rate (μ , h^{-1}), at concentration x , d is the upper-limit corresponding to the growth rate of the untreated algae and b is the slope of the curve around EC_{50} .

2.4.2. Mixture modelling approaches

Procedures of the two mixture modelling approaches (isobole model and MIXTOX tool) are described in detail in Dupraz et al. (2018). Therefore, only the concepts and basic principles that are useful to understand the results and discussion are described in §2.4.2.1 and §2.4.2.2 below.

2.4.2.1. Isobole model

Predictions from the two reference isobole models, CA and IA, were calculated for each mixture based on the concentration-response parameters of the single chemicals. The detailed procedure is described in Dupraz et al. (2018). Briefly, when the CA model did not provide an acceptable fit to the experimental data, more advanced Hewlett and Vølund models (Hewlett, 1969; Vølund, 1992), which are extensions of the CA model, were tested. For each mixture ray, the experimental (observed) Toxic Unit (TU) value was calculated using Eq. 2 (Loewe and Muischnek, 1926),

$$\sum_{i=1}^n \frac{z_i}{ECx_i} = 1 \quad (2)$$

where, z_i is the concentration of the chemical i in the mixture giving $x\%$ effect and ECx_i is the effective concentration yielding the same effect as the mixture, in our case, EC_{50i} for a 50% inhibition.

The quotient z_i/ECx_i corresponds to the dimensionless TU value that quantifies the relative contribution to toxicity of the individual chemical i in the mixture of n chemicals. The expected TU value is 1 TU. The reciprocal of the TU value is equivalent to MDR (model deviation ratio), which is useful to discriminate significant interactions from simple additivity. Hence, as proposed in Belden et al. (2007) and Cedergreen (2014), a factor of two between observed and expected TU value was used as a threshold to discriminate biologically significant interactions: $TU < 0.5$ is suggestive of synergy, values in the range $0.5 \leq TU \leq 2$ are not suggestive of antagonism or synergy (additivity), and a $TU > 2$ is suggestive of antagonism.

The TU approach was also used to calculate the concentrations of single pesticides in a 50:50% mixture that theoretically resulted in growth rate inhibitions of 25%, 50% and 75% (§2.3.2) according to the CA model. Individual concentrations of substances x and y in the mixture were calculated so that the corresponding $\Sigma TU_{50:50}$ values were equal to 0.5, 1 and 1.5 TU, as described in Eq. 3 (example with 1 TU, for further details see Dupraz et al., 2018),

$$\frac{x}{EC_{50}X} + \frac{y}{EC_{50}Y} = 1 \quad (3)$$

where x and y are the concentrations of the substances X and Y in the binary mixtures, and $EC_{50}X$ and $EC_{50}Y$ are their respective EC_{50} s (Loewe and Muischnek, 1926). Since the two substances in a 50:50% mixture ratio contribute equally to the mixture toxicity, individual quotients are thus equal to 0.5 TU. Knowing the EC_{50} s for each substance as well as the desired inhibition effect, in this case 50% (corresponding to 1 TU), makes it possible to calculate x and y .

2.4.2.2. MIXTOX tool

The MIXTOX tool provides an alternative approach to the Hewlett and Vølund isobole models and is implemented in an Excel[®] macro developed by Jonker et al. (2005). Similarly to the isobole model, prediction of the mixture toxicity according to CA and IA models can be computed using knowledge of concentration-response parameters of the single chemicals (Eq. 1). The detailed procedure is described in Dupraz et al. (2018). Briefly, when the CA model did not provide an acceptable fit to the experimental data, deviations from the CA or IA models were described using the synergism/antagonism (S/A) model and the dose ratio/dose level-dependent deviation (DR/DL) models. Mathematical derivations of the models and interpretations are given in Jonker et al. (2005).

2.5. Measurements on microalgae

2.5.1. Microalgal growth

2.5.1.1. Microplate reader

Microalgal growth was measured every 24 h, during the light phase using chlorophyll fluorescence. Microplates were analysed using a SAFIRE microplate reader (TECAN) with the *XFluor4beta* Excel[®] macro as software. Excitation/emission wavelengths were: 450/684 nm (10.0 nm bandwidth), nine reads were performed per well from the bottom, with an integration time of 20.0 μ s. Each microplate was shaken for 20 s before the reading, using an Orbis Plus (Mikura Ltd) microplate shaker in orbital mode. For each well, the growth rate was calculated for each species and substance combination tested over the 96-h exposure period, using the Eq. 4,

$$\mu = \frac{\ln(F_t - F_0)}{t} \quad (4)$$

where F_t is the fluorescence (a.u.) of the well at t (h), μ (h^{-1}) is the growth rate and F_0 the initial fluorescence intensity at $t = 0$ h.

2.5.1.2. Flow cytometry

Fresh microalgal samples (0.50 mL, 2.3.2) were run on a BD-Accuri C6 flow cytometer (Becton Dickinson Accuri™) equipped with blue (488 nm) and red (640 nm) lasers, detectors of forward (FSC) and side (SSC) light scatter, and four fluorescence detectors: 530 ± 15 nm (FL1), 585 ± 20 nm (FL2), > 670 nm (FL3) and 675 ± 12.5 nm (red laser, FL4). FL1 vs FL4 channel density plots were used to determine cell density for both microalgal species, and each species was gated to avoid counting non-microalgal particles. For each culture flask, the growth rate was calculated for the species and substance/s tested over the 96-h exposure period, with Eq. 5,

$$\mu = \frac{\ln(C_t - C_0)}{t} \quad (4)$$

where C_t is the cell density (cell mL^{-1}) of the culture at t (h), μ (h^{-1}) is the growth rate, and C_0 the initial cell density at $t = 0$ h.

2.5.2. Photosystem II effective quantum yield

Photosystem II effective quantum yield (operational yield: ϕ'_M) was measured by Pulse Amplitude Modulated (PAM) fluorescence using an Aquapen-C AP-C 100 fluorometer (Photon System Instruments®, Drasov, Czech Republic). Measurements were made using fresh 2.00-mL microalgal samples (§2.3.2) in light adapted conditions (light intensity of the culture chamber). Three measurements were performed for each culture and the mean of these values taken.

2.5.3. Physiological endpoints

The selected physiological endpoints were followed using specific fluorescent dyes. As mentioned in the introduction, some pesticides can affect the fluorescence of microalgal pigments. As a result, the fluorescence of fresh exposed cells (unstained, FL1 or FL2_{fresh}; supplementary material: Table S6) can significantly differ from controls. Therefore, to avoid any bias, FL1 or FL2_{fresh} values were systematically subtracted from the fluorescence values of stained cells: FL1_{FDA}, FL1_{BOD}, FL1_{DIB}, FL1_{DCF} and FL2_{DHE}, for cells stained with FDA, BODIPY^{505/515}, DiBAC₄(3), H₂DCFDA and dihydroethidium, respectively (supplementary material: Tables S7 and S8).

2.5.3.1. Metabolic activity

Metabolic activity of microalgal cells was estimated using the fluorescein-based lipophilic dye fluorescein diacetate (FDA, ThermoFisher Invitrogen™) which makes it possible to evaluate changes in the

cell metabolic activity by comparing the mean fluorescence intensity (MFI) of metabolically active (FDA+) cells (Seoane et al., 2014).

FDA-derived fluorescence was detected by the FL1 detector on a logarithmic scale.

The protocol for metabolic activity determination was adapted from Prado et al. (2009). Preliminary experiments were carried out to determine the optimal FDA concentration and incubation time to use for *T. lutea* and *S. marinoi* cultures, using cultures heated to 80°C as a positive control. Fresh microalgal samples (0.50 mL, §2.3.2) were incubated with FDA at final concentrations of 2.50 (*T. suecica*, 0.005% DMSO) or 5.00 µM (*S. marinoi*, 0.01% DMSO) for 10 min in the dark at room temperature before analysis.

2.5.3.2. Relative intracellular lipid content

The green lipophilic fluorochrome BODIPY^{505/515} (ThermoFisher Invitrogen™) was used to estimate the relative intracellular lipid content, changes of which can be detected by comparing the MFI of marked cells (BOD+).

BODIPY⁵⁰⁵⁻⁵¹⁵-derived fluorescence was detected by the FL1 detector on a logarithmic scale.

The protocol for relative intracellular lipid content was adapted from Brennan et al. (2012) and Dupraz et al. (2016) and preliminary experiments were carried out to determine the optimal BODIPY^{505/515} concentration and incubation time to use for *T. lutea* and *S. marinoi* cultures. For both species, samples containing 0.50 mL of microalgal culture (§2.3.2) were incubated with 0.48 µM (0.01% DMSO) BODIPY^{505/515} and left in the dark at room temperature for 10 min before analysis.

2.5.3.3. Cytoplasmic membrane potential

In this study, the cytoplasmic membrane potential of microalgal cells was monitored using the slow-response potential-sensitive probe, DiBAC₄(3) (ThermoFisher Invitrogen™). Changes in cytoplasmic membrane potential can be detected by comparing the MFI of marked cells (DiBAC+). The DiBAC₄(3)-derived fluorescence was detected with the FL1 detector on a logarithmic scale.

Staining protocols from Prado et al. (2012) and Seoane et al. (2017) were adapted. Preliminary experiments were carried out to determine the optimal DiBAC₄(3) concentration and incubation time to use for *T. lutea* and *S. marinoi* cultures. Briefly, microalgal samples (0.50 mL, §2.3.2) were stained with 0.97 µM of DiBAC₄(3) (0.01% DMSO) and analysis was performed after 10 min incubation in the dark at room temperature.

2.5.3.4. Reactive oxygen species (ROS)

The fluorescent dyes 2',7'-dichlorodihydrofluorescein diacetate (H₂DCFDA or DCFH-DA, Sigma-Aldrich®) and dihydroethidium (or hydroethidine, DHE, ThermoFisher Invitrogen™) were both used to measure ROS content in microalgal cells.

Differences in intracellular ROS content can be assessed by comparing MFI of positively-marked cells with H₂DCFDA (DCF+). The FL1 detector was used to detect H₂DCFDA-derived fluorescence. The staining protocol was adapted from Stachowski-Haberkorn et al. (2013). Preliminary experiments were carried out to determine the optimal H₂DCFDA concentration and incubation time to use for *T. lutea* and *S. marinoi* cultures by exposing test cultures to 1.00 mM H₂O₂ (final concentration) as a positive control. Briefly, samples containing microalgal cells (0.50 mL, 2.3.2) were incubated with 60.0 μM H₂DCFDA (0.01% DMSO) and kept in the dark at room temperature for 30 min before analysis.

Differences in superoxide anion content can be monitored by comparing the MFI of positively-marked cells with DHE (DHE+). The DHE-derived fluorescence was detected with the FL2 detector on a logarithmic scale. The staining protocol was adapted from Prado et al. (2012). Preliminary experiments were carried out to determine the optimal DHE concentration and incubation time to use for *T. lutea* and *S. marinoi* cultures by exposing test cultures to 1.00 mM H₂O₂ (final concentration) as a positive control. Fresh microalgal samples (0.50 mL, §2.3.2) were incubated with DHE at final concentrations of 15.85 μM (0.01% DMSO) for 30 min in the dark at room temperature before analysis.

3. Results

3.1. Toxicity of single substances

In the microplate experiments, prior to determining the interactive effects of the eight selected binary mixtures, concentration-response experiments were performed for each chemical singly to determine their EC₅₀ on both microalgal species (Table 1). In general, EC₅₀s later determined in the binary mixture experiments (supplementary material: Table S9) were close to those determined in preliminary experiments. The most toxic pesticide for both microalgal species was diuron, with EC₅₀s around 2 μg L⁻¹ for *T. lutea* and 10 μg L⁻¹ for *S. marinoi*. The herbicide isoproturon and fungicide spiroxamine were also relatively toxic to both species, with EC₅₀s around 10 and 5 μg L⁻¹, respectively, for *T. lutea* and ranging from 13 to 20 μg L⁻¹ and 35 and 45 μg L⁻¹ for *S. marinoi*.

EC₅₀s determined in the culture flask experiments were generally lower than those obtained in microplates (supplementary material: Table S6). For *T. lutea*, while a very similar EC₅₀ was obtained for diuron (2.21 ± 0.48 μg L⁻¹), a nearly two-fold lower EC₅₀ was obtained for isoproturon (~5-6 μg L⁻¹) and the value for spiroxamine was six-fold lower (0.83 ± 0.07 μg L⁻¹) in the flask than in the microplate. For *S. marinoi*, a similar EC₅₀ was obtained for metazachlor (289 ± 48.0 μg L⁻¹), but for diuron (5.74 ± 0.28 μg L⁻¹) and spiroxamine (15.1 ± 0.79 μg L⁻¹) the values were roughly halved in the flasks while the EC₅₀ for isoproturon was four- to six-fold lower (between 3.22 ± 0.17 and 5.17 ± 0.33 μg L⁻¹).

3.2. Binary mixtures in microplates

Six and seven binary mixtures were tested on *T. lutea* and *S. marinoi*, respectively, to investigate their interactive effect.

In general, the same main interaction effect was determined by both mixture modelling approaches, except for two mixtures (one for each species). The following interactions were determined using the statistical procedure described in Dupraz et al., 2018.

For *T. lutea*, according to the isobole model and with respect to CA model predictions, one mixture was additive (ISO+AZO), two were antagonistic (ISO+QUI and ISO+SPI), two were synergistic (ISO+DIU and SPI+QUI), and one was partly antagonistic and partly synergistic (SPI+CHL-M) (Figure 1, Table 2). Regarding the results obtained with the MIXTOX tool, the CA model always gave better predictions than the IA model: compared to CA model predictions, two mixtures were synergistic (ISO+DIU and SPI+QUI), while the four others were antagonistic (Table 2).

Regarding *S. marinoi*, the isobole model described one additive interaction (ISO+DIU), five cases of antagonism (ISO+AZO, ISO+QUI, ISO+SPI, SPI+QUI and SPI+MET) and one case of synergism (ISO+MET) (Figure 2, Table 2). Contrary to what was observed with *T. lutea*, the IA model gave better predictions for four mixtures out of seven: the mixture ISO+DIU behaved according to the CA model predictions, while the ISO+QUI and ISO+MET mixtures resulted in antagonism and synergism, respectively, compared with CA model predictions. Compared with IA model predictions, three mixtures (ISO+AZO, ISO+SPI and SPI+MET) induced antagonism, while the mixture SPI+QUI was synergistic (Table 2).

When looking at the TU values for these mixtures (Table 2, supplementary material: Table S9), only two mixtures, tested on *S. marinoi*, should be considered as biologically significant ($TU > 2$): ISO+AZO ($TU_{25:75} = 2.10 \pm 0.22$) and ISO+SPI ($TU_{50:50} = 2.19 \pm 0.15$ and $TU_{25:75} = 2.76 \pm 0.30$).

Following these experiments, three mixtures were selected to further explore their effects on the physiology of the two microalgae: ISO+DIU, as an example of concentration additivity; ISO+SPI, as an example of potential antagonism, and ISO+MET (tested on *S. marinoi*), as a case of potential synergy.

3.3. Binary mixtures in culture flasks

The toxicity of the three selected combinations to the two marine microalgae was examined more closely in larger volumes. Culture flask experiments were run for each single substance and the 50:50% mixture ratio. Effects on growth, PSII quantum yield and several physiological functions were explored using PAM-fluorescence and flow cytometry.

3.3.1. Mixture of isoproturon and diuron

The inhibition of growth rate (GRi%) induced by isoproturon and diuron singly, or in a mixture, was close to expected for the haptophyte *T. lutea* (supplementary material: Table S6). Regarding the effects on

ϕ'_M , similar effects were obtained at equivalent GRi% for isotroturon, diuron and their mixture, with decreases ranging from 17% to 34% (Figure 3). Effects of isotroturon were concentration-dependent. Among the other parameters measured by flow cytometry, only BODIPY^{505/515} (FL1_{BOD}) and dihydroethidium (FL2_{DHE}) induced significant effects relative to the controls: decreases ranging from 23% to 39% were observed in FL1_{BOD}.

For the diatom *S. marinoi*, significant effects with respect to the controls (Figure 3) were observed whatever the endpoint measured. The GRi% obtained after exposure to diuron was close to expected, while slightly higher for isotroturon and the mixture. Regarding impacts on PSII quantum yield, significant decreases in ϕ'_M , ranging from 8% to 19% were observed. Significant decreases in FL1_{FDA} were observed for all treatments tested, ranging from 19% to 41%. Interestingly, marked decreases on FL1_{BOD} (from 37% to 62%) were induced by isotroturon, diuron and their mixture. For isotroturon and diuron, the decreases observed were concentration-dependent for all Σ TU tested. Regarding FL1_{DIB} and FL1_{DCF}, all treatments induced a significant decrease of about 15–24% and 10–22%, respectively, with no significant difference detected between them. Finally, all treatments except ISO 1.5 TU and DIU 0.5 TU significantly increased FL2_{DHE}, from 10% to 22%.

3.3.2. Mixture of isotroturon and spiroxamine

Regarding the effects of this mixture on *T. lutea*, the GRi% was relatively close to the one expected (supplementary material: Table S6). Isotroturon induced significant decreases in ϕ'_M , ranging from 17% to 29%, while only the highest concentration of spiroxamine (6%) and all mixture conditions (from 12% to 24%) resulted in significant decreases (Figure 4). Both FL1_{FDA} and FL1_{BOD} increased significantly upon exposure to spiroxamine at 1 and 1.5 TU, with increases ranging from 83% to 123% and 123% to 145%, respectively. No effects of isotroturon or the mixture were observed for these parameters. FL1_{DIB} decreased significantly after exposure to 1 (32%) and 1.5 TU (39%) isotroturon, while a 94% increase in FL1_{DIB} was induced by spiroxamine at 1.5 TU. Both spiroxamine and the mixture caused significant increases in FL1_{DCF} at all Σ TU tested, ranging from 72% to 293% for spiroxamine and 91% to 126% for the mixture. Significant decreases of 23% and 26% in FL2_{DHE} were observed after exposure to 1 and 1.5 TU of isotroturon, respectively.

For the diatom *S. marinoi*, only isotroturon induced the expected GRi%. At 0.5 TU, spiroxamine induced almost no effect on growth rate (6% GRi), while at 1 TU, an 84% GRi was observed, and 100% inhibition was obtained upon exposure to 1.5 TU (supplementary material: Table S6). The effects induced by the mixture were much lower than expected, as 10%, 19% and 32% GRi were induced at 0.5, 1 and 1.5 TU, respectively. Small, but significant decreases were observed on ϕ'_M : at 1 (12%) and 1.5 TU (14%) for isotroturon; and at 0.5 (9%) and 1.5 TU (10%) for the mixture (Figure 4). *S. marinoi* cells exposed to spiroxamine showed an increase in FL1_{FDA} of 24% at 0.5 TU and 35% at 1.5 TU. Both isotroturon and the mixture significantly decreased FL1_{BOD}: the lowest decrease (26%) was caused by the mixture at 0.5 TU, while the highest (62%) was induced by 1.5 TU isotroturon. Spiroxamine, in contrast, led to 23 and 75%

increases in FL1_{BOD} after exposure to 0.5 and 1 TU, respectively. A 246% increase in FL1_{DIB} was observed after exposure to 1 TU spiroxamine. Decreases of 25%, 30% and 24% were observed on FL1_{DCF} after exposure to 0.5 TU isoproturon and the mixture at 0.5 and 1 TU, respectively. Finally, spiroxamine increased FL1_{DCF} and FL2_{DHE} by 33% and 44% at 1 TU, respectively.

3.3.3. Mixture of isoproturon and metazachlor

This mixture was only tested on *S. marinoi*. For isoproturon, and to an even greater extent for the mixture, GRi values induced were far higher than expected, especially for the lowest concentrations, with 17% and 45% differences at 0.5 TU, and 24% and 31% differences at 1 TU, respectively (supplementary material: Table S6). For metazachlor, the GRi was 18% higher than expected at 0.5 TU and 20% lower than expected at 1.5 TU. All conditions, except the lowest concentration of metazachlor, induced significant decreases in ϕ'_M , ranging from 14% to 34% (Figure 5B). At equivalent Σ TU, the mixture induced significantly higher decreases in ϕ'_M than isoproturon or metazachlor alone, reaching dramatic inhibition rates. Decreases in FL1_{FDA} were only observed at 0.5 TU (21%) and 1 TU (25%) of isoproturon (Figure 5A). Highly contrasting effects were obtained on FL1_{BOD}: isoproturon and the mixture induced similar decreases, ranging from 46% to 65%, while metazachlor caused remarkable increases ranging from 239% to 295%. Significant effects on FL1_{DIB} were only observed for metazachlor, with increases ranging from 41% to 71%. Isoproturon induced significant decreases in FL1_{DCF} at all concentrations tested, as well as the mixture at 1.5 TU, ranging from 21% to 30%, while metazachlor induced a 16% increase at 0.5 TU. Finally, all tested concentrations of metazachlor and the mixture at 0.5 and 1 TU induced increases in FL2_{DHE} ranging from 15% to 42%.

4. Discussion

4.1. Toxicity of single substances in microplates and culture flasks

EC₅₀s of isoproturon and diuron determined in this study (Table 1, supplementary table: Table S6 and S9) were consistent with previously reported values (Arzul et al., 2006; Bao et al., 2011). For the other substances tested in this study, EC₅₀s also appear to be consistent with those reported in the Pesticides Properties DataBase (PPDB) and Pesticide Ecotoxicity DataBase (PEDB) (Lewis et al., 2016; U.S. EPA, 2018).

As pointed out in the results section, EC₅₀s determined in culture flasks (supplementary material: Table S6) were two- to six-fold lower than those in microplates, indicating a higher toxicity for exposed microalgae (Table 1 and supplementary material: Table S9). These discrepancies are probably due to the different characteristics of the materials composing microplates and culture flasks (plastic vs. glass), as well as to the different growth endpoints used to assess impacts on growth in the two exposure systems (cell density in culture flasks vs chlorophyll fluorescence in microplates) as previously discussed in Dupraz et al. (2019). Some chemicals are known to modify the fluorescence of microalgal pigments (Prado et al., 2011; Stachowski-Haberkorn et al., 2013), as also shown in the present study by the measurement of FL1 and FL2 fluorescence

of fresh microalgal cells (supplementary material: Table S6). Therefore, the modification of pigment content and/or fluorescence might have biased growth rate measurement in microplates, leading to an underestimation of toxicity. This phenomenon was therefore considered when analysing the FL1 and FL2 fluorescence of the marked cells (§2.5.3.5).

4.2. Interactive effects of binary pesticide mixtures

The toxicity and interaction effects of binary mixtures of pesticides have been examined in several previous studies. In the review by Cedergreen (2014), none of the 120 binary mixtures of pesticides, tested on plants or algae, had significant synergy. On the contrary, a large proportion resulted in antagonism, while a few behaved according to concentration additivity. In another study considering the growth of the freshwater alga *Pseudokirchneriella subcapitata* (now called *Raphidocelis subcapitata*), the pesticides metsulfuron-methyl, terbuthylazine and bentazone tested in binary combinations with the organophosphate malathion did not result in significant interactions compared with CA predictions (Munkegaard et al., 2008). Recently, Mansano et al. (2017) reported synergy resulting from the mixture of diuron and carbofuran, a carbamate insecticide, on the growth of the microalga *Raphidocelis subcapitata*, compared with the CA model predictions.

In the present study, almost all mixtures tested were responsible for significant interaction effects compared with the predictions of the reference models and results of the statistical tests performed. However, following the recommendations of Belden et al. (2007) and Cedergreen (2014), only two mixtures tested in microplates, ISO+AZO and ISO+SPI tested on *S. marinoi*, showed biologically significant antagonism, deviating by a factor of two or more ($TU > 2$) from the expected TU value. Although not deviating by as much compared with CA predictions, the mixture ISO+MET on *S. marinoi* had observed TU values close to 0.5 for two mixture ratios in the microplate experiments ($TU_{50:50} = 0.68 \pm 0.03$ and $TU_{25:75} = 0.66 \pm 0.06$, supplementary material: Table S9). Tested in culture flasks, the 50:50% ISO+MET mixture was responsible for a four-fold higher toxicity compared with the CA model prediction ($TU_{50:50} = 0.26 \pm 0.06$, Table 3). Therefore, it appears reasonable to consider the synergism observed for this mixture as biologically significant.

4.3. Effects of the single substances on physiological parameters and implications for microalgal cells

Significant decreases in ϕ'_M were expected and observed for both species (Figures 3, 4 and 5) when exposed to the PSII inhibitors isoproturon and diuron. It was not the case of spiroxamine and metazachlor, which target the biosynthesis of sterols and VLCFAs (Table 1), through inhibition of the enzymes Δ^{14} -sterol reductase (ERG24) and VLCFA-FAE1 synthase, respectively (Debieu et al., 2000; Götz and Böger, 2004). This was confirmed for spiroxamine (Figure 4), however, metazachlor induced a slight decrease in ϕ'_M at 1 and 1.5 TU (Figure 5B). A moderate inhibition of photosynthesis was previously reported on *Chlamydomonas*

reinhardtii cells exposed to high concentrations of S-metolachlor (Korkaric et al., 2015), although the mechanism of action responsible is not known.

Following the light phase of photosynthesis, the Calvin cycle permits production of many precursors including those used in lipid biosynthesis (Masojídek et al., 2004). A reduced production of these precursors, and therefore lipids, might have occurred due to reduced photosynthetic efficiency, and could explain the large decreases observed in FL1_{BOD} after exposure to isotroturon and diuron (Figures 3, 4 and 5). Indeed, in a study conducted on two strains of *T. lutea* (a wild and an oleaginous strain), the authors demonstrated that BODIPY fluorescence was correlated with reserve lipid content, measured by gas chromatography coupled with a flame induction detector (da Costa et al., 2017). In contrast, spiroxamine (especially for *T. lutea*, Figure 4) and metazachlor (for *S. marinoi*, Figure 5A) both caused large increases in FL1_{BOD}. Microalgae are known to produce reserve lipids under stressful conditions as a result of reduced cell division, e.g., under nitrogen limitation conditions (Zhu et al., 2016; da Costa et al., 2017). In the study from Vallotton et al. (2008), S-metolachlor inhibited cell division of *Scenedesmus vacuolatus*, leading to subsequent cell enlargement. Hence, metazachlor, and possibly spiroxamine, could have induced reserve lipid accumulation, as indicated by high increases in FL1_{BOD} (Figures 4 and 5A), due to cell division inhibition: GRi% ranged from 43% to 54% for metazachlor on *S. marinoi*, and between 38% and 66% for spiroxamine on *T. lutea* (supplementary material: Table S6).

Another consequence of photosynthesis inhibition is the potential accumulation of intracellular ROS, as previously described in many studies (Knauert and Knauer, 2008; Prado et al., 2012; Stachowski-Haberkorn et al., 2013; Esperanza et al., 2015; Dupraz et al., 2016). In the present study, significant effects, measured using either H₂DCFDA or dihydroethidium, were observed after exposure to all individual substances (Figures 3, 4 and 5A). However, for *S. marinoi*, isotroturon and diuron induced a decrease in FL1_{DCF}, but an increase in FL2_{DHE} (Figure 3). As pointed out in Kalyanaraman et al. (2012), H₂DCFDA first requires esterases to be converted into H₂DCF, which reacts with ROS to form DCFH that is then oxidized to form the fluorescent dichlorofluorescein (DCF). In this study, the fluorescent probe FDA was used to measure the metabolic activity of non-specific esterases: decreased esterase activity was observed after exposure to isotroturon and diuron for *S. marinoi* and was concomitant with decreases observed in FL1_{DCF} values (Figures 3 and 5A). Therefore, variations in FL1_{DCF} observed with H₂DCFDA could be partly due to fluctuations in esterase activity, rather than modification in ROS content. Consequently, results obtained with H₂DCFDA should be interpreted carefully and dihydroethidium, which does not require prior esterase activity, could be a more reliable probe for measurement of intracellular ROS content. With respect to these findings, isotroturon and diuron seem to have increased ROS content, as measured by FL2_{DHE}, in *S. marinoi* cells (Figure 3) but not in *T. lutea*, for which variable results were obtained (Figures 3 and 4). Both spiroxamine and metazachlor increased ROS content (Figures 4 and 5) for the two microalgal species. Accumulation of intracellular ROS in microalgal cells could be related to a general stress caused by these toxicants (Mallick and Mohn, 2000), and often lead to significant damages to cell constituents and cytoplasmic membranes (Knauert and Knauer, 2008; Stoiber et al., 2013).

Finally, both isoproturon and diuron induced a decrease in FL1_{DIB} values for *S. marinoi* (Figure 3), reflecting cytoplasmic membrane hyperpolarization. As both sterols and VLCFAs are important constituents of cell membranes (Cassagne et al., 1994; Haines, 2001; Ohvo-Rekilä et al., 2002), significant effects on the cytoplasmic membrane were expected upon exposure to spiroxamine and metazachlor: significant depolarization of cell membranes was observed, as indicated by increased FL1_{DIB} values, which could have led to membrane disruption and increased cell permeability. As mentioned above, ROS are involved in oxidative damage to cell membrane constituents. Hence, complementary analysis of lipid peroxidation (Cheloni and Slaveykova, 2013; Melegari et al., 2013) might make it possible to link the effects observed on the cytoplasmic membrane potential with those observed on intracellular ROS content.

The analysis of the physiological effects of the single substances furthered our understanding of their toxic MOA, a necessary step to further investigate the interactive effects of the tested mixtures.

4.4. Interactive effects of pesticides on microalgal physiology

It is first important to point out that, even though concentrations of the substances singly and in mixtures were theoretically calculated to induce 25%, 50% or 75% GRi (expected Σ TU = 0.5, 1 and 1.5 TU, respectively), the expected GRi% was not always attained (Table 3). These discrepancies were partly due to very different slopes of the concentration-response relationships of the tested chemicals, as well as differences between the toxicity observed in microplates and in culture flasks. This issue was the most important for the mixture of isoproturon and spiroxamine (Figure 4), and to a lesser extent for the mixture of isoproturon and metazachlor (Figure 5). Thus, it was decided to only compare the effects observed on microalgal physiology among treatments with equivalent GRi% (Table 3).

The mixture made up of isoproturon and diuron resulted in concentration additivity for the two microalgal species in both microplates and culture flasks (Figures 1 and 2, Tables 2 and 3). When comparing the effects caused by the single substances with those caused by the mixture (Figure 3), almost no significant differences were observed at equivalent Σ TU. As expected, the effects caused by the mixture corroborate the principle of the concentration addition model potency (Loewe and Muischnek, 1926): both isoproturon and diuron can be viewed as dilutions of each other, only differing in potency. Therefore, it was shown that the concentration addition model is not only applicable to growth, but to the whole set of parameters measured in this study.

Regarding the two other mixtures, as the MOA of the mixed substances were different, effects on the measured physiological functions were less predictable. In general, isoproturon and spiroxamine had opposite effects on the monitored parameters. The effects of their mixture on ϕ'_M was probably only due to isoproturon, as spiroxamine had almost no effect on PSII quantum yield for either species (Figure 4). The decrease in relative lipid content for *S. marinoi* exposed to the mixture of isoproturon and spiroxamine was probably related to photosynthesis inhibition caused by isoproturon, as already mentioned above. To sum up, only a few significant effects were observed for the mixture, with generally the same trends as for isoproturon, except

for FL1_{DCF} in *T. lutea*. This reflects important differences in the molecular structures targeted by isotroturon and spiroxamine, which could partly explain the strong antagonism observed for *S. marinoi* (TU_{50:50} = 3.10 ± 0.71, Table 3).

The effect of the mixture of isotroturon and metazachlor on *S. marinoi* was probably the most interesting, as it resulted in biologically significant synergy. The effects obtained on the PSII quantum yield were particularly notable: significantly higher decreases in ϕ'_M were observed for the mixture compared with the two single chemicals at all Σ TU tested (Figure 5B). High decreases in FL1_{BOD}, ranging from 46% to 64%, were also observed for all concentrations tested, which corroborates the above-mentioned hypothesis of a link between PSII inhibition and reduced lipid content. Only a few significant effects were observed for the other measured parameters. As photosynthesis is a vital process for microalgal cells, we can therefore hypothesize that the synergy resulting from this mixture was mainly due to the higher inhibition of photosynthesis observed.

Hypotheses can be made to explain the higher decrease in ϕ'_M observed for the mixture of isotroturon and metazachlor. Metazachlor significantly affected the cytoplasmic membrane potential, as shown by the depolarization induced in exposed cells. This is consistent with the expected MOA of this substance, as VLCFAs are important constituents of cell membranes (Cassagne et al., 1994). However, the link between membrane depolarization and an increase in its general permeability is not clear. Additional analyses of the lipid composition, microscope observations, and isotroturon uptake measurements of affected and unaffected microalgal cells are all potential future avenues to further investigate this hypothesis.

Elsewhere, the morphology of thylakoid membranes, where photosynthesis takes place, could also be affected by a decreased VLCFA content, potentially disrupting the normal functioning of PSII (Schneiter and Kohlwein, 1997; Millar et al., 1998; Thakkar et al., 2013). In addition, a recent study demonstrated that chloroplast division was also decreased in *Arabidopsis thaliana* plants treated with an inhibitor of VLCFA synthesis (Nobusawa and Umeda, 2012). In the light of these findings, it appears reasonable to suggest that the inhibition of VLCFAs induced by metazachlor could somehow have disrupted the photosynthetic apparatus. This disruption could have enhanced the toxic effects of isotroturon on PSII and subsequently caused the observed synergy.

Phenylureas and chloroacetamides are among the most frequently detected pesticides in European watercourses (Moschet et al., 2014), and are also often found in coastal waters (Watts et al., 2000; Munaron et al., 2012; Cruzeiro et al., 2015). Hence, the synergy resulting from the combination of these substances might pose a potential threat to the environment.

5. Conclusion

The eight binary mixtures of pesticides tested on two marine microalgae *T. lutea* and *S. marinoi* in the microplate assay displayed varying responses. The majority of them showed interactions that were in the range

of additivity and only two mixtures (isoproturon + azoxystrobin or spiroxamine) exhibited biologically significant antagonism on *S. marinoi*.

The mixture of isoproturon and metazachlor resulted in a significant synergistic effect towards *S. marinoi* in culture flasks: a four-fold higher toxicity than predicted by the CA model was observed.

A further investigation of three selected mixtures, illustrating potential examples of additivity (isoproturon + diuron), antagonism (isoproturon + spiroxamine) and synergy (isoproturon + metazachlor), was performed using flow cytometry and PAM-fluorescence.

Very contrasted effects were induced by isoproturon and spiroxamine, highlighting their different intracellular targets, which could potentially explain the significant antagonism observed on *S. marinoi*.

Finally, the significant synergy observed for the mixture of isoproturon and metazachlor tested on *S. marinoi* could be mainly due to a combined effect of the single substances on the photosynthetic apparatus, enhancing photosynthesis inhibition.

As these substances, and others belonging to the same chemical family, are among the most frequently detected in European watercourses and coastal waters, further investigation of their effects in combination should be carried out.

6. Acknowledgements

This study was carried out with financial support from the French National Research Agency (ANR) in the framework of the Investments for the Future program, within the Cluster of Excellence COTE (ANR-10-LABX-45). We also want to thank Nathalie Coquillé and Julien Rouxel for their technical assistance, as well as Philippe Soudant for his helpful advice. We thank Helen McCombie for the English correction. We also thank two anonymous reviewers for their comments, which helped us to improve the quality of this manuscript.

7. References

- Altenburger, R., Bödeker, W., Faust, M., Horst Grimme, L., 1990. Evaluation of the isobologram method for the assessment of mixtures of chemicals. *Ecotoxicol. Environ. Saf.* 20, 98–114. doi:10.1016/0147-6513(90)90049-B
- Arzul, G., Quiniou, F., Carrie, C., 2006. In vitro test-based comparison of pesticide-induced sensitivity in marine and freshwater phytoplankton. *Toxicol. Mech. Methods* 16, 431–437. doi:10.1080/15376520600698717
- Bao, V.W.W., Leung, K.M.Y., Kwok, K.W.H., Zhang, A.Q., Lui, G.C.S., 2008. Synergistic toxic effects of zinc pyrethrin and copper to three marine species: Implications on setting appropriate water quality criteria. *Mar. Pollut. Bull.* 57, 616–623. doi:10.1016/j.marpolbul.2008.03.041
- Bao, V.W.W., Leung, K.M.Y., Qiu, J.W., Lam, M.H.W., 2011. Acute toxicities of five commonly used antifouling booster biocides to selected subtropical and cosmopolitan marine species. *Mar. Pollut. Bull.* 62, 1147–1151. doi:10.1016/j.marpolbul.2011.02.041

- Beardall, J., Raven, J.A., 2016. Carbon acquisition by microalgae, in: Borowitzka, M.A., Beardall, J., Raven, J.A. (Eds.), *The Physiology of Microalgae*. Springer International Publishing, pp. 89–99. doi:10.1007/978-3-319-24945-2_4
- Belden, J.B., Gilliom, R.J., Lydy, M.J., 2007. How well can we predict the toxicity of pesticide mixtures to aquatic life? *Integr. Environ. Assess. Manag.* 3, 364–372. doi:10.1002/ieam.5630030307
- Bergtold, M., Dohmen, G.P., 2011. Biomass or growth rate endpoint for algae and aquatic plants: relevance for the aquatic risk assessment of herbicides. *Integr. Environ. Assess. Manag.* 7, 237–47. doi:10.1002/ieam.136
- Bliss, C.I., 1939. The Toxicity Of Poisons Applied Jointly. *Ann. Appl. Biol.* 26, 585–615. doi:10.1111/j.1744-7348.1939.tb06990.x
- Brennan, L., Blanco Fernández, A., Mostaert, A.S., Owende, P., 2012. Enhancement of BODIPY 505/515 lipid fluorescence method for applications in biofuel-directed microalgae production. *J. Microbiol. Methods* 90, 137–143. doi:10.1016/j.mimet.2012.03.020
- Caquet, T., Roucaute, M., Mazzella, N., Delmas, F., Madigou, C., Farcy, E., Burgeot, T., Allenou, J.-P.P., Gabellec, R., 2013. Risk assessment of herbicides and booster biocides along estuarine continuums in the Bay of Vilaine area (Brittany, France). *Environ. Sci. Pollut. Res.* 20, 651–666. doi:10.1007/s11356-012-1171-y
- Cassagne, C., Lessire, R., Bessoule, J.J., Moreau, P., Creach, A., Schneider, F., Sturbois, B., 1994. Biosynthesis of very long chain fatty acids in higher plants. *Prog. Lipid Res.* 33, 55–69. doi:10.1016/0163-7827(94)90009-4
- Cedergreen, N., 2014. Quantifying synergy: A systematic review of mixture toxicity studies within environmental toxicology. *PLoS One* 9, e96580. doi:10.1371/journal.pone.0096580
- Cedergreen, N., Kamper, A., Streibig, J.C., 2006. Is prochloraz a potent synergist across aquatic species? A study on bacteria, daphnia, algae and higher plants. *Aquat. Toxicol.* 78, 243–252. doi:10.1016/j.aquatox.2006.03.007
- Cedergreen, N., Kudsk, P., Mathiassen, S.K., Streibig, J.C., 2007. Combination effects of herbicides on plants and algae: do species and test systems matter? *Pest Manag. Sci.* 63, 282–295. doi:10.1002/ps.1353
- Cedergreen, N., Svendsen, C., Backhaus, T., 2013. Toxicity Prediction of Chemical Mixtures, in: *Encyclopedia of Environmental Management*. Taylor & Francis, New York. doi:10.1081/E-EEM-120046684
- Chapman, R.L., 2013. Algae: The world's most important “plants”-an introduction. *Mitig. Adapt. Strateg. Glob. Chang.* 18, 5–12. doi:10.1007/s11027-010-9255-9
- Cheloni, G., Slaveykova, V.I., 2013. Optimization of the C11-BODIPY581/591 Dye for the Determination of Lipid Oxidation in *Chlamydomonas reinhardtii* by Flow Cytometry. *Cytometry* 83, 952–961. doi:10.1002/cyto.22338
- Coquillé, N., Ménard, D., Rouxel, J., Dupraz, V., Éon, M., Pardon, P., Budzinski, H., Morin, S., Parlanti, É., Stachowski-Haberkorn, S., 2018. The influence of natural dissolved organic matter on herbicide toxicity to marine microalgae is species-dependent. *Aquat. Toxicol.* 198, 103–117. doi:10.1016/j.aquatox.2018.02.019
- Cruzeiro, C., Rocha, E., Pardal, M.Â., Rocha, M.J., 2015. Uncovering seasonal patterns of 56 pesticides in surface coastal waters of the Ria Formosa lagoon (Portugal), using a GC-MS method. *Int. J. Environ. Anal. Chem.* 95, 1370–1384. doi:10.1080/03067319.2015.1100724

- da Costa, F., Le Grand, F., Quéré, C., Bougaran, G., Cadoret, J.P., Robert, R., Soudant, P., 2017. Effects of growth phase and nitrogen limitation on biochemical composition of two strains of *Tisochrysis lutea*. *Algal Res.* 27, 177–189. doi:10.1016/j.algal.2017.09.003
- de Zwart, D., Posthuma, L., 2005. Complex mixture toxicity for single and multiple species. *Environ. Toxicol. Chem.* 24, 2665. doi:10.1897/04-639R.1
- Debenest, T., Pinelli, E., Coste, M., Silvestre, J., Mazzella, N., Madigou, C., Delmas, F., 2009. Sensitivity of freshwater periphytic diatoms to agricultural herbicides. *Aquat. Toxicol.* 93, 11–17. doi:10.1016/j.aquatox.2009.02.014
- Debieu, D., Bach, J., Arnold, A., Brousset, S., Gredt, M., Taton, M., Rahier, A., Malosse, C., Leroux, P., 2000. Inhibition of Ergosterol Biosynthesis by Morpholine, Piperidine, and Spiroketalamine Fungicides in *Microdochium nivale*: Effect on Sterol Composition and Sterol $\Delta 8 \rightarrow \Delta 7$ -Isomerase Activity. *Pestic. Biochem. Physiol.* 67, 85–94. doi:10.1006/pest.2000.2485
- Dupraz, V., Coquillé, N., Ménard, D., Sussarellu, R., Haugarreau, L., Stachowski-Haberkorn, S., 2016. Microalgal sensitivity varies between a diuron-resistant strain and two wild strains when exposed to diuron and irgarol, alone and in mixtures. *Chemosphere* 151, 241–252. doi:10.1016/j.chemosphere.2016.02.073
- Dupraz, V., Stachowski-Haberkorn, S., Ménard, D., Limon, G., Akcha, F., Budzinski, H., Cedergreen, N., 2018. Combined effects of antifouling biocides on the growth of three marine microalgal species. *Chemosphere*. doi:10.1016/j.chemosphere.2018.06.139
- Dupraz, V., Stachowski-Haberkorn, S., Wicquart, J., Tapie, N., Budzinski, H., Akcha, F., 2019. Demonstrating the need for chemical exposure characterisation in a microplate test system: toxicity screening of sixteen pesticides on two marine microalgae. *Chemosphere* 221, 278–291. doi:10.1016/j.chemosphere.2019.01.035
- Ebenezer, V., Ki, J.-S.S., 2013. Quantification of toxic effects of the herbicide metolachlor on marine microalgae *Ditylum brightwellii* (Bacillariophyceae), *Prorocentrum minimum* (Dinophyceae), and *Tetraselmis suecica* (Chlorophyceae). *J. Microbiol.* 51, 136–139. doi:10.1007/s12275-013-2114-0
- Esperanza, M., Cid, Á., Herrero, C., Rioboo, C., 2015. Acute effects of a prooxidant herbicide on the microalga *Chlamydomonas reinhardtii*: Screening cytotoxicity and genotoxicity endpoints. *Aquat. Toxicol.* 165, 210–21. doi:10.1016/j.aquatox.2015.06.004
- European Chemicals Agency, 2018. ECHA [WWW Document]. URL <https://echa.europa.eu/fr/home>
- González-Pleiter, M., Gonzalo, S., Rodea-Palomares, I., Leganés, F., Rosal, R., Boltes, K., Marco, E., Fernández-Piñas, F., 2013. Toxicity of five antibiotics and their mixtures towards photosynthetic aquatic organisms: Implications for environmental risk assessment. *Water Res.* 47, 2050–2064. doi:10.1016/j.watres.2013.01.020
- González-Pleiter, M., Rioboo, C., Reguera, M., Abreu, I., Leganés, F., Cid, Á., Fernández-Piñas, F., 2017. Calcium mediates the cellular response of *Chlamydomonas reinhardtii* to the emerging aquatic pollutant Triclosan. *Aquat. Toxicol.* 186, 50–66. doi:10.1016/j.aquatox.2017.02.021
- Götz, T., Böger, P., 2004. The very-long-chain fatty acid synthase is inhibited by chloroacetamides. *Zeitschrift für Naturforsch. - Sect. C J. Biosci.* 59, 549–553.
- Guillard, R.R.L., 1975. Culture of Phytoplankton for Feeding Marine Invertebrates, in: Smith, W.L., Chanley, M.H. (Eds.), *Culture of Marine Invertebrate Animals SE - 3*. Springer US, Boston, MA, pp. 29–60. doi:10.1007/978-1-4615-8714-9_3
- Guillard, R.R.L., Ryther, J.H., 1962. Studies of marine planktonic diatoms. I. *Cyclotella nana* Hustedt and

Detonula confervacea (Cleve) Gran. Can. J. Microbiol. 8, 229–239. doi:10.1139/m62-029

- Haines, T.H., 2001. Do sterols reduce proton and sodium leaks through lipid bilayers? Prog. Lipid Res. 40, 299–324. doi:10.1016/S0163-7827(01)00009-1
- Hlaili, A.S., Niquil, N., Legendre, L., 2014. Planktonic food webs revisited: Reanalysis of results from the linear inverse approach. Prog. Oceanogr. 120, 216–229. doi:10.1016/j.pocean.2013.09.003
- Holmes, C.M., Brown, C.D., Hamer, M., Jones, R., Maltby, L., Posthuma, L., Silberhorn, E., Teeter, J.S., Warne, M.S.J., Weltje, L., 2018. Prospective aquatic risk assessment for chemical mixtures in agricultural landscapes. Environ. Toxicol. Chem. 37, 674–689. doi:10.1002/etc.4049
- ISO 10253:2016, 2016. Water quality - Marine algal growth inhibition test with *Skeletonema sp.* and *Phaeodactylum tricorutum*. International Organization for Standardization, Geneva, Switzerland.
- ISO 8692:2012, 2012. Water quality - Fresh water algal growth inhibition test with unicellular green algae. Geneva, Switzerland.
- Jonker, M.J., Svendsen, C., Bedaux, J.J.M., Bongers, M., Kammenga, J.E., 2005. Significance testing of synergistic/antagonistic, dose level-dependent, or dose ratio-dependent effects in mixture dose-response analysis. Environ. Toxicol. Chem. 24, 2701. doi:10.1897/04-431R.1
- Junghans, M., Backhaus, T., Faust, M., Scholze, M., Grimme, L.H., 2003. Predictability of combined effects of eight chloroacetanilide herbicides on algal reproduction. Pest Manag. Sci. 59, 1101–1110. doi:10.1002/ps.735
- Kalyanaraman, B., Darley-Usmar, V., Davies, K.J.A., Dennery, P.A., Forman, H.J., Grisham, M.B., Mann, G.E., Moore, K., Roberts, L.J., Ischiropoulos, H., 2012. Measuring reactive oxygen and nitrogen species with fluorescent probes: Challenges and limitations. Free Radic. Biol. Med. 52, 1–6. doi:10.1016/j.freeradbiomed.2011.09.030
- Knauert, S., Knauer, K., 2008. The role of reactive oxygen species in copper toxicity to two freshwater green algae. J. Phycol. 44, 311–319. doi:10.1111/j.1529-8817.2008.00471.x
- Korkaric, M., Behra, R., Fischer, B.B., Junghans, M., Eggen, R.I.L., 2015. Multiple stressor effects in *Chlamydomonas reinhardtii* – Toward understanding mechanisms of interaction between effects of ultraviolet radiation and chemical pollutants. Aquat. Toxicol. 162, 18–28. doi:10.1016/j.aquatox.2015.03.001
- Koutsaftis, A., Aoyama, I., 2006. The interactive effects of binary mixtures of three antifouling biocides and three heavy metals against the marine algae *Chaetoceros gracilis*. Environ. Toxicol. 21, 432–439. doi:10.1002/tox.20202
- Larsbo, M., Sandin, M., Jarvis, N., Etana, A., Kreuger, J., 2016. Surface Runoff of Pesticides from a Clay Loam Field in Sweden. J. Environ. Qual. 45, 1367. doi:10.2134/jeq2015.10.0528
- Lewis, K.A., Tzilivakis, J., Warner, D.J., Green, A., 2016. An international database for pesticide risk assessments and management. Hum. Ecol. Risk Assess. An Int. J. 22, 1050–1064. doi:10.1080/10807039.2015.1133242
- Loewe, S., Muischnek, H., 1926. Combined effects I Announcement - Implements to the problem. Naunyn. Schmiedeberg's. Arch. Exp. Pathol. Pharmacol. 114, 313–326.
- Magdaleno, A., Saenz, M.E., Juárez, A.B., Moreton, J., 2015. Effects of six antibiotics and their binary mixtures on growth of *Pseudokirchneriella subcapitata*. Ecotoxicol. Environ. Saf. 113, 72–78. doi:10.1016/j.ecoenv.2014.11.021

- Magnusson, M., Heimann, K., Negri, A.P., 2008. Comparative effects of herbicides on photosynthesis and growth of tropical estuarine microalgae. *Mar. Pollut. Bull.* 56, 1545–52. doi:10.1016/j.marpolbul.2008.05.023
- Mallick, N., Mohn, F.H., 2000. Reactive oxygen species: Response of algal cells. *J. Plant Physiol.* 157, 183–193. doi:10.1016/S0176-1617(00)80189-3
- Mansano, A.S., Moreira, R.A., Dornfeld, H.C., Freitas, E.C., Vieira, E.M., Sarmiento, H., Rocha, O., Seleguim, M.H.R., 2017. Effects of diuron and carbofuran and their mixtures on the microalgae *Raphidocelis subcapitata*. *Ecotoxicol. Environ. Saf.* 142, 312–321. doi:10.1016/j.ecoenv.2017.04.024
- Marie, D., Simon, N., Vaultot, D., 2005. Phytoplankton Cell Counting by Flow Cytometry. *Algal Cult. Tech.* 1, 253–556.
- Masojídek, J., Koblížek, M., Torzillo, G., 2004. Photosynthesis in Microalgae, in: *Handbook of Microalgal Culture*. Blackwell Publishing Ltd, Oxford, UK, pp. 20–39. doi:10.1002/9780470995280.ch2
- Melegari, S.P., Perreault, F., Costa, R.H.R., Popovic, R., Matias, W.G., 2013. Evaluation of toxicity and oxidative stress induced by copper oxide nanoparticles in the green alga *Chlamydomonas reinhardtii*. *Aquat. Toxicol.* 142–143, 431–440. doi:10.1016/j.aquatox.2013.09.015
- Millar, a a, Wrisher, M., Kunst, L., 1998. Accumulation of very-long-chain fatty acids in membrane glycerolipids is associated with dramatic alterations in plant morphology. *Plant Cell* 10, 1889–1902. doi:10.1105/tpc.10.11.1889
- Mohr, S., Berghahn, R., Feibicke, M., Meinecke, S., Ottenströer, T., Schmiedling, I., Schmiediche, R., Schmidt, R., 2007. Effects of the herbicide metazachlor on macrophytes and ecosystem function in freshwater pond and stream mesocosms. *Aquat. Toxicol.* 82, 73–84. doi:10.1016/j.aquatox.2007.02.001
- Mohr, S., Feibicke, M., Berghahn, R., Schmiediche, R., Schmidt, R., 2008. Response of plankton communities in freshwater pond and stream mesocosms to the herbicide metazachlor. *Environ. Pollut.* 152, 530–542. doi:10.1016/j.envpol.2007.07.010
- Moschet, C., Wittmer, I., Simovic, J., Junghans, M., Piazzoli, A., Singer, H., Stamm, C., Leu, C., Hollender, J., 2014. How a complete pesticide screening changes the assessment of surface water quality. *Environ. Sci. Technol.* 48, 5423–5432. doi:10.1021/es500371t
- Munaron, D., Tapie, N., Budzinski, H., Andral, B., Gonzalez, J.-L.L., 2012. Pharmaceuticals, alkylphenols and pesticides in Mediterranean coastal waters: Results from a pilot survey using passive samplers. *Estuar. Coast. Shelf Sci.* 114, 82–92. doi:10.1016/j.ecss.2011.09.009
- Munkegaard, M., Abbaspoor, M., Cedergreen, N., 2008. Organophosphorous insecticides as herbicide synergists on the green algae *Pseudokirchneriella subcapitata* and the aquatic plant *Lemna minor*. *Ecotoxicology* 17, 29–35. doi:10.1007/s10646-007-0173-x
- Nagai, T., De Schamphelaere, K.A.C., 2016. The effect of binary mixtures of zinc, copper, cadmium, and nickel on the growth of the freshwater diatom *Navicula pelliculosa* and comparison with mixture toxicity model predictions. *Environ. Toxicol. Chem.* 35, 2765–2773. doi:10.1002/etc.3445
- Nobusawa, T., Umeda, M., 2012. Very-long-chain fatty acids have an essential role in plastid division by controlling Z-ring formation in *Arabidopsis thaliana*. *Genes to Cells* 17, 709–719. doi:10.1111/j.1365-2443.2012.01619.x
- Ochoa-Acuña, H.G., Bialkowski, W., Yale, G., Hahn, L., 2009. Toxicity of soybean rust fungicides to freshwater algae and *Daphnia magna*. *Ecotoxicology* 18, 440–6. doi:10.1007/s10646-009-0298-1
- Ohvo-Rekilä, H., Ramstedt, B., Leppimäki, P., Peter Slotte, J., 2002. Cholesterol interactions with

phospholipids in membranes. *Prog. Lipid Res.* 41, 66–97. doi:10.1016/S0163-7827(01)00020-0

- Papadakis, E.N., Tsaboula, A., Kotopoulou, A., Kintzikoglou, K., Vryzas, Z., Papadopoulou-Mourkidou, E., 2015. Pesticides in the surface waters of Lake Vistonis Basin, Greece: Occurrence and environmental risk assessment. *Sci. Total Environ.* 536, 793–802. doi:10.1016/j.scitotenv.2015.07.099
- Pérez, G.L., Solange, V.M., Miranda, L., 2011. Effects of herbicide glyphosate and glyphosate-based formulations on aquatic ecosystems, in: Kortekamp, A. (Ed.), *Herbicides and Environment*. InTech, Argentina, pp. 343–368.
- Prado, R., García, R., Rioboo, C., Herrero, C., Abalde, J., Cid, A., 2009. Comparison of the sensitivity of different toxicity test endpoints in a microalga exposed to the herbicide paraquat. *Environ. Int.* 35, 240–247. doi:10.1016/j.envint.2008.06.012
- Prado, R., Rioboo, C., Herrero, C., Cid, Á., 2011. Characterization of cell response in *Chlamydomonas moewusii* cultures exposed to the herbicide paraquat: Induction of chlorosis. *Aquat. Toxicol.* 102, 10–17. doi:10.1016/j.aquatox.2010.12.013
- Prado, R., Rioboo, C., Herrero, C., Suárez-Bregua, P., Cid, Á., 2012. Flow cytometric analysis to evaluate physiological alterations in herbicide-exposed *Chlamydomonas moewusii* cells. *Ecotoxicology* 21, 409–420. doi:10.1007/s10646-011-0801-3
- Ravier, I., Haouisee, E., Clément, M., Seux, R., Briand, O., 2005. Field experiments for the evaluation of pesticide spray-drift on arable crops. *Pest Manag. Sci.* 61, 728–736. doi:10.1002/ps.1049
- Rioboo, C., González-Barreiro, Ó., Abalde, J., Cid, Á., 2011. Flow cytometric analysis of the encystment process induced by paraquat exposure in *Haematococcus pluvialis* (Chlorophyceae). *Eur. J. Phycol.* 46, 89–97. doi:10.1080/09670262.2011.561775
- Ritz, C., Baty, F., Streibig, J.C., Gerhard, D., 2015. Dose-Response Analysis Using R. *PLoS One* 10, e0146021. doi:10.1371/journal.pone.0146021
- Ritz, C., Streibig, J.C., 2005. Bioassay analysis using R. *J. Stat. Softw.* 12, 1–22. doi:10.18637/jss.v012.i05
- Schneider, R., Kohlwein, S.D., 1997. Organelle structure, function, and inheritance in yeast: A role for fatty acid synthesis? *Cell* 88, 431–434. doi:10.1016/S0092-8674(00)81882-6
- Seoane, M., Esperanza, M., Rioboo, C., Herrero, C., Cid, Á., 2017. Flow cytometric assay to assess short-term effects of personal care products on the marine microalga *Tetraselmis suecica*. *Chemosphere* 171, 339–347. doi:10.1016/j.chemosphere.2016.12.097
- Seoane, M., Rioboo, C., Herrero, C., Cid, Á., 2014. Toxicity induced by three antibiotics commonly used in aquaculture on the marine microalga *Tetraselmis suecica* (Kyllin) Butch. *Mar. Environ. Res.* 101, 1–7. doi:10.1016/j.marenvres.2014.07.011
- Sjollema, S.B., MartínezGarcía, G., van der Geest, H.G., Kraak, M.H.S., Booij, P., Vethaak, A.D., Admiraal, W. Hazard and risk of herbicides for marine microalgae. *Environ. Pollut.* 187, 106–111. doi:10.1016/j.envpol.2013.12.019
- Sørensen, H., Cedergreen, N., Skovgaard, I.M., Streibig, J.C., 2007. An isobole-based statistical model and test for synergism/antagonism in binary mixture toxicity experiments. *Environ. Ecol. Stat.* 14, 383–397. doi:10.1007/s10651-007-0022-3
- Southwick, L.M., Appelboom, T.W., Fouss, J.L., 2009. Runoff and leaching of metolachlor from Mississippi River alluvial soil during seasons of average and below-average rainfall. *J. Agric. Food Chem.* 57, 1413–1420. doi:10.1021/jf802468m

- Stachowski-Haberkorn, S., Jérôme, M., Rouxel, J., Khelifi, C., Rincé, M., Burgeot, T., 2013. Multigenerational exposure of the microalga *Tetraselmis suecica* to diuron leads to spontaneous long-term strain adaptation. *Aquat. Toxicol.* 140–141, 380–388. doi:10.1016/j.aquatox.2013.06.016
- Stoiber, T.L., Shafer, M.M., Armstrong, D.E., 2013. Induction of reactive oxygen species in *Chlamydomonas reinhardtii* in response to contrasting trace metal exposures. *Environ. Toxicol.* 28, 516–523. doi:10.1002/tox.20743
- Thakkar, M., Randhawa, V., Wei, L., 2013. Comparative responses of two species of marine phytoplankton to metolachlor exposure. *Aquat. Toxicol.* 126, 198–206. doi:10.1016/j.aquatox.2012.10.002
- U.S. EPA, 2018. Pesticide Ecotoxicity Database [WWW Document]. URL <http://www.ipmcenters.org/Ecotox/index.cfm> (accessed 6.27.18).
- Vallotton, N., Moser, D., Eggen, R.I.L., Junghans, M., Chèvre, N., 2008. S-metolachlor pulse exposure on the alga *Scenedesmus vacuolatus*: Effects during exposure and the subsequent recovery. *Chemosphere* 73, 395–400. doi:10.1016/j.chemosphere.2008.05.039
- Vallotton, N., Price, P.S., 2016. Use of the Maximum Cumulative Ratio As an Approach for Prioritizing Aquatic Coexposure to Plant Protection Products: A Case Study of a Large Surface Water Monitoring Database. *Environ. Sci. Technol.* 50, 5286–5293. doi:10.1021/acs.est.5b06267
- Vendrell, E., Ferraz, D.G. de B., Sabater, C., Carrasco, J.M., 2009. Effect of glyphosate on growth of four freshwater species of phytoplankton: a microplate bioassay. *Bull. Environ. Contam. Toxicol.* 82, 538–42. doi:10.1007/s00128-009-9674-z
- Watts, D.W., Novak, J.M., Johnson, M.H., Stone, K.C., 2000. Storm flow export of metolachlor from a coastal plain watershed. *J. Environ. Sci. Heal. - Part B Pestic. Food Contam. Agric. Wastes* 35, 175–186. doi:10.1080/03601230009373262
- Wauchope, R.D., Ahuja, L.R., Arnold, J.G., Bingner, R., Lowrance, R., Van Genuchten, M.T., Adams, L.D., 2003. Software for pest-management science: Computer models and databases from the United States Department of Agriculture - Agricultural Research Service. *Pest Manag. Sci.* 59, 691–698. doi:10.1002/ps.682
- Zhang, X., Luo, Y., Goh, K.S., 2018. Modeling spray drift and runoff-related inputs of pesticides to receiving water. *Environ. Pollut.* 234, 48–58. doi:10.1016/j.envpol.2017.11.032
- Zhu, L.D., Li, Z.H., Hiltunen, E., 2016. Strategies for Lipid Production Improvement in Microalgae as a Biodiesel Feedstock. *Biomed Res. Int.* 2016, 7–9. doi:10.1155/2016/8792548

Figure captions

Figure 1: Isobolograms resulting from the binary mixtures of isoproturon with diuron (A), azoxystrobin (B), spiroxamine (D) or quinoxyfen (E), as well as spiroxamine with quinoxyfen (C) or chlorpyrifos-methyl (F), tested on *Tisochrysis lutea* in microplates. The points represent the $EC_{50} \pm 2$ standard-error (s.e.). The straight solid line is the CA isobole; the dot-dashed line is the IA isobole; the curved solid line (when displayed) is the best fitting isobole model when there is a significant interaction.

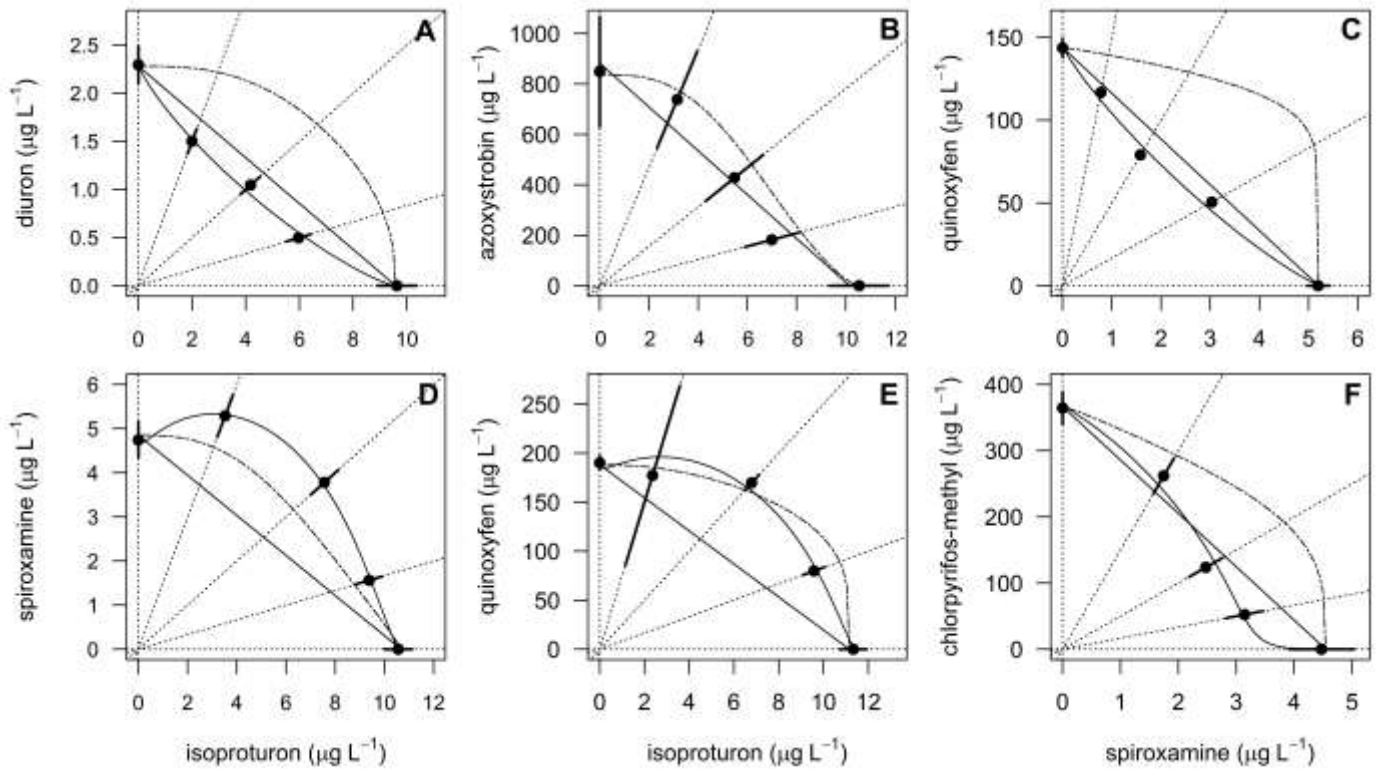


Figure 2: Isobolograms resulting from the binary mixtures of isoproturon with diuron (A), azoxystrobin (B), spiroxamine (D), quinoxyfen (E) or metazachlor (G), as well as spiroxamine with quinoxyfen (C) or metazachlor (F), tested on *Skeletonema marinoi* in microplates. The points represent the $EC_{50} \pm 2$ standard-error (s.e.). The straight solid line is the CA isobole; the dot-dashed line is the IA isobole; the curved solid line (when displayed) is the best fitting isobole model when there is a significant interaction.

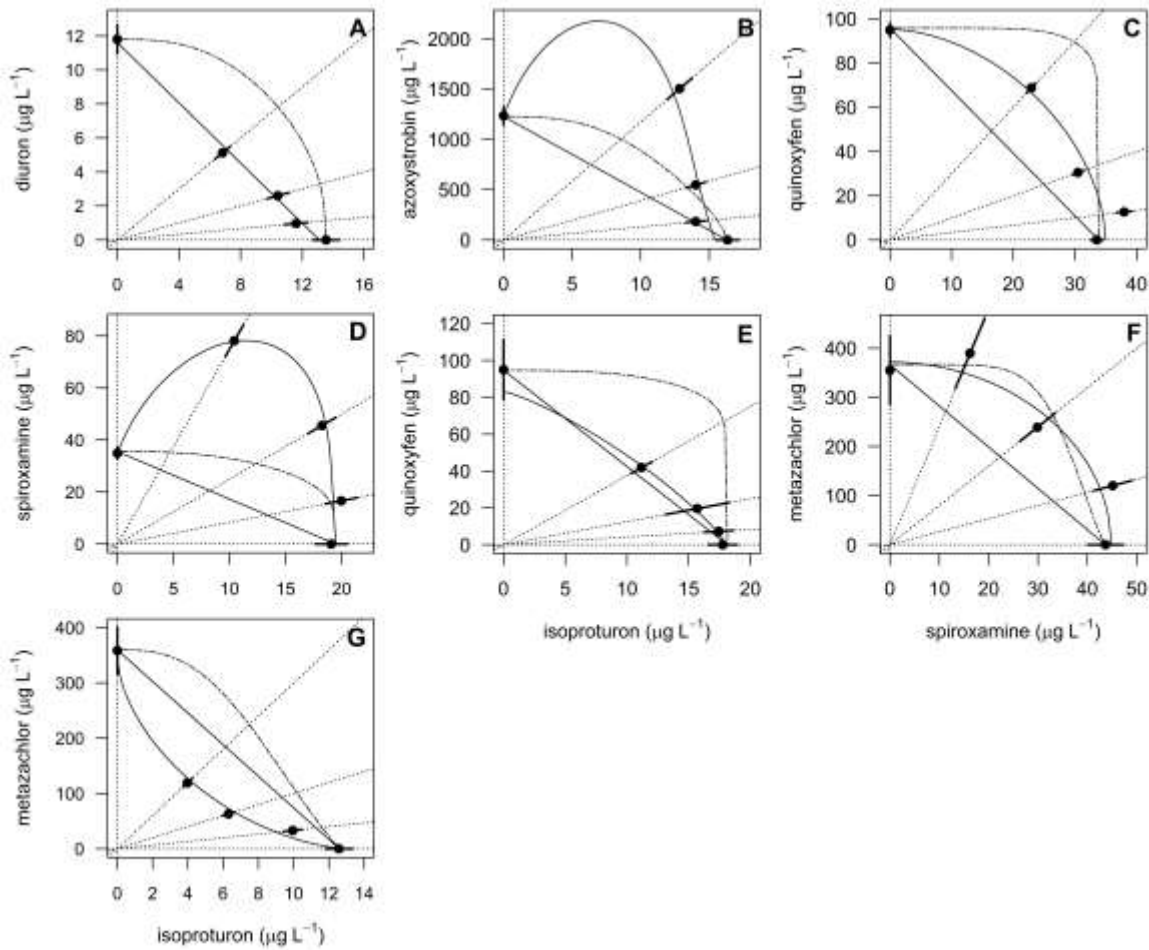


Figure 3: Effects, measured as the % of variation compared with solvent controls, of isoproturon (ISO), diuron (DIU) and their binary mixtures (MIX) on the PSII quantum yield (ϕ'_M), esterase activity ($FL1_{FDA}$), relative lipid content ($FL1_{BOD}$), cytoplasmic membrane potential ($FL1_{DIB}$) and ROS content ($FL1_{DCF}$ and $FL2_{DHE}$) in *T. lutea* and *S. marinoi*. Concentrations are expressed as TUs. Only significant effects relative to solvent controls are displayed; letters denote significant differences between treatments (ANOVA, $p < 0.05$).

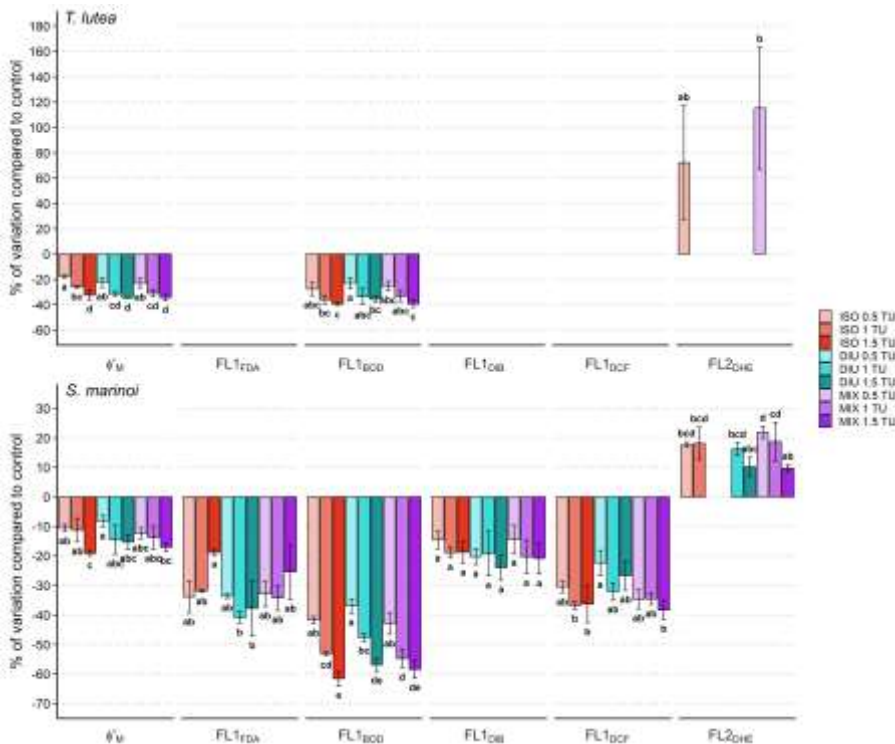


Figure 4: Effects, measured as the % of variation compared with solvent controls, of isotreturon (ISO), spiroxamine (SPI) and their binary mixtures (MIX) on the PSII quantum yield (ϕ'_M), esterase activity (FL1_{FDA}), relative lipid content (FL1_{BOD}), cytoplasmic membrane potential (FL1_{DIB}) and ROS content (FL1_{DCF} and FL2_{DHE}) in *T. lutea* and *S. marinoi*. Concentrations are expressed as TUs. Only significant effects relative to solvent controls are displayed; letters denote significant differences between treatments (ANOVA, $p < 0.05$).

*For *S. marinoi*, effects of SPI 1.5 TU are not displayed due to total inhibition of microalgal growth.

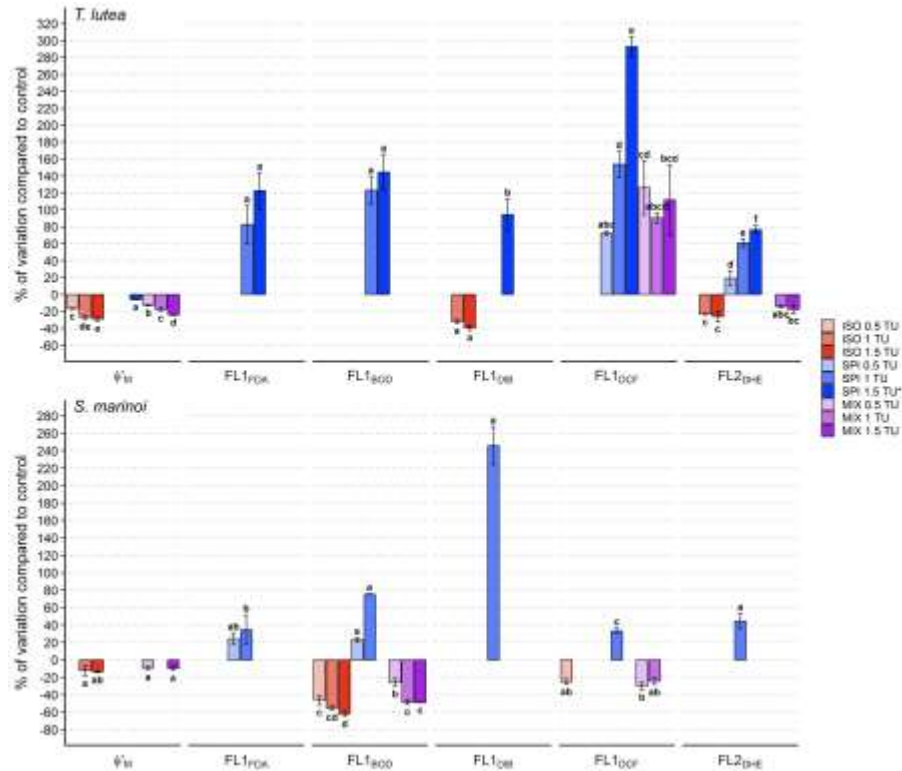


Figure 5: Effects, measured as the % of variation compared with solvent controls, of isotreturon (ISO), metazachlor (MET) and their binary mixture (MIX), on (A) the PSII quantum yield* (ϕ'_M) esterase activity (FL1_{FDA}), relative lipid content (FL1_{BOD}), cytoplasmic membrane potential (FL1_{DIB}) and ROS content (FL1_{DCF} and FL2_{DHE}) in *S. marinoi*. *A focus on the quantum yield is also shown in part B. Concentrations are expressed in TUs. Only significant effects relative to solvent controls are displayed; letters denote significant differences between treatments (ANOVA, $p < 0.05$).

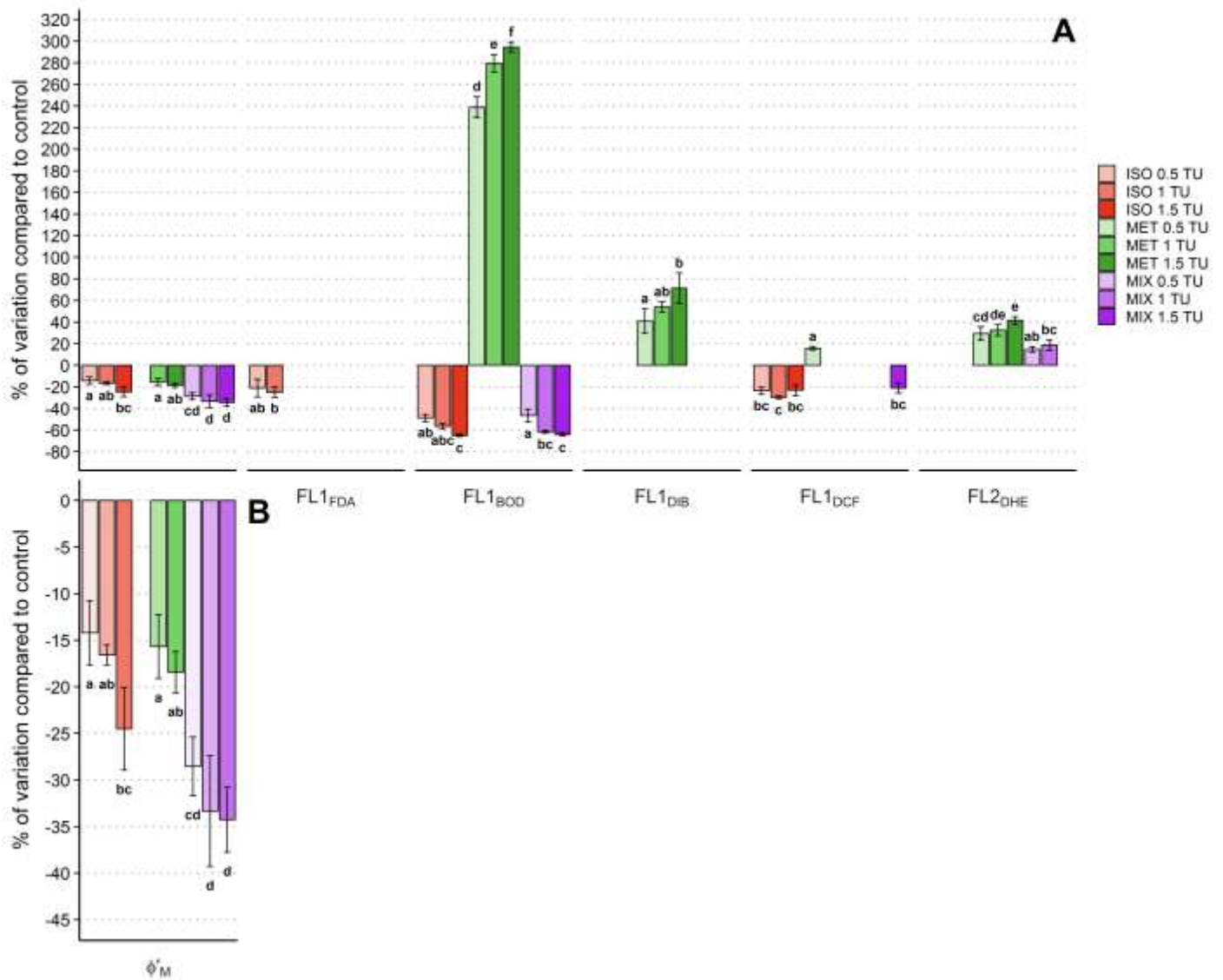


Table 1. Pesticides tested in this study, their chemical families, mode of action (PPDB, Lewis et al., 2016; ANSES, 2018) and EC_{50} s (\pm 95% confidence interval, in $\mu\text{g L}^{-1}$). Concentration-response curves are available in the supplementary material (Figure S2 and S3). *n.d.* signifies that no EC_{50} could be calculated in the range tested.

Class	Substance	Chemical Family	Mode of action (MOA)	$EC_{50}^{(1)}$ ($\mu\text{g L}^{-1}$)	
				<i>T. lutea</i>	<i>S. marinoi</i>
Biocide⁽²⁾	diuron	phenylurea	inhibition of photosynthesis at photosystem II	2.20 \pm 0.071	10.3 \pm 0.80
	isoproturon	phénylurea		13.0 \pm 6.76	18.3 \pm 1.29
Herbicide	metazachlor	chloroacetamide	inhibition of elongase and geranylgeranyl pyrophosphate (GGPP)	<i>n.d.</i>	370 \pm 43.2
Insecticide	chlorpyrifos-methyl	organophosphate	inhibition of acetylcholine esterase (AChE)	406 \pm 6.33	<i>n.d.</i>
	azoxystrobin	strobilurine	inhibition of the respiratory chain at the level of Complex III	624 \pm 207	1504 \pm 386
Fungicide	quinoxifen	quinoleine	disruption of early cell signalling events	320 \pm 7.10	68.8 \pm 33.0
	spiroxamine	morpholine	inhibition of sterol biosynthesis	5.04 \pm 1.37	45.7 \pm 44.6

⁽¹⁾ EC_{50} s were determined using strictly the same procedure as described in §2.3.1.

⁽²⁾ These two substances were previously used as herbicides but are now only permitted as biocides.

Table 2. Summary of mixture interaction on *T. lutea* and *S. marinoi*. For the isobole model, the best fitting model (BFM) is displayed beside the main interaction effect (EFF.) compared with the CA model; interaction parameters are displayed in the case of antagonism or synergism: λ for Hewlett model or η_1 and η_2 for Vølund model. For MIXTOX, the BFM is displayed beside the interaction effect, compared with the best reference model (BRM, CA or IA); interaction parameters are displayed in the case of antagonism or synergism: a for S/A or a and b for DR/DL models; For each model, the p -value displayed corresponds to the F -test performed to determine whether the extended model provides a significantly better fit ($p < 0.05$) than the less complex model.

Mixture	<i>T. lutea</i>				<i>S. marinoi</i>			
	TU _{50:50} ⁽¹⁾	Isobole BFM ⁽²⁾ / EFF. ⁽³⁾ Int. param. \pm s.e. p -value	MIXTOX Best Reference Model (BRM)	BFM / EFF. Int. param. p -value	TU _{50:50}	Isobole BFM / EFF. Int. param. \pm s.e. p -value	MIXTOX Best Reference Model (BRM)	BFM / EFF. Int. param. p -value
ISO + DIU	0.87 \pm 0.09	Hewlett / SYN. $\lambda = 1.24 \pm 0.06$ $p < 10^{-3}$	CA	S/A / SYN. $a = -0.67$ $p < 10^{-3}$	0.95 \pm 0.06	CA / ADD.	CA	CA / ADD.
ISO + MET					0.68 \pm 0.03	Hewlett / SYN. $\lambda = 1.57 \pm 0.06$ $p < 10^{-3}$	CA	S/A / SYN. $a = -1.67$ $p < 10^{-3}$

ISO + AZO	1.01 ± 0.28	CA / ADD.	CA	DR _{CA} / ANT. a = 2.19 b _{ISO} = -2.59 p < 10 ⁻³	1.31 ± 0.05	Vølund / ANT. η ₁ = 0.80 ± 0.57 η ₂ = 7.7 ± 1.84 p < 10 ⁻³	IA	DR _{IA} / ANT. a = 5.49 b _{ISO} = -7.67 p < 10 ⁻³
ISO + QUI	1.52 ± 0.09	Vølund / ANT. η ₁ = 0.66 ± 0.10 η ₂ = 3.84 ± 0.65 p < 10 ⁻³	CA	DL _{CA} / ANT. a = 0.74 b _{ISO} = -0.62 p < 10 ⁻³	1.10 ± 0.11	Hewlett / ANT. λ = 0.81 ± 0.072 p = 0.04	CA	DL _{CA} / ANT. a = 3.27 b _{DL} = 0.82 p < 10 ⁻³
ISO + SPI	1.48 ± 0.10	Vølund / ANT. η ₁ = 0.66 ± 0.10 η ₂ = 4.50 ± 0.89 p < 10 ⁻³	CA	DR _{CA} / ANT. a = 2.34 b _{ISO} = -1.66 p < 10 ⁻³	2.19 ± 0.15	Vølund / ANT. η ₁ = 0.97 ± 0.06 η ₂ = 8.57 ± 0.90 p < 10 ⁻³	IA	DR _{IA} / ANT. a = 11.77 b _{ISO} = -15.83 p < 10 ⁻³
SPI + QUI	0.86 ± 0.01	Hewlett / SYN. λ = 1.18 ± 0.03 p < 10 ⁻³	CA	DL _{CA} / SYN. a = -0.14 b _{SPI} = -2.04 p < 10 ⁻³	1.19 ± 0.03	Hewlett / ANT. λ = 0.56 ± 0.03 p < 10 ⁻³	IA	DR _{IA} / SYN. a = -11.92 b _{SPI} = 14.37 p < 10 ⁻³
SPI + CHL-M	0.90 ± 0.18	Vølund / ANT.- SYN. η ₁ = 2.18 ± 0.58 η ₂ = 0.37 ± 0.14 p = 10 ⁻³	CA	DR _{CA} / ANT. a = 1.60 b _{SPI} = -3.14 p = 0.006				
SPI + MET					1.42 ± 0.11	Hewlett / ANT. λ = 0.51 ± 0.09 p < 10 ⁻³	IA	S/A / ANT. a = 0.80 p < 10 ⁻³

⁽¹⁾ TU for other mixture ratios (75:25% and 25:75%), as well as individual EC₅₀s for single chemicals are available in supplementary material: Table S9). TU < 0.5 is suggestive of synergy, values in the range 0.5 ≤ TU ≤ 2 are not suggestive of antagonism or synergy (additivity), and a TU > 2 is suggestive of antagonism.

⁽²⁾ BFM: Best fitting model, either a reference model (CA or IA) or a more complex model, Hewlett or S/A (one interaction parameter), Vølund or DR/DL (two interaction parameters).

⁽³⁾ EFF.: Main interaction effect noted for the mixture, either additivity (ADD.), antagonism (ANT.) or synergism (SYN.). Biologically significant interactions (TU < 0.5 or TU > 2) are in **bold**.

Table 3. Comparison of growth rate inhibition percentages (GRi%) and observed TU_{50:50} (\pm 95% confidence interval) obtained for the three single substances tested in culture flasks and their binary mixtures for both microalgal species. The ‘TU’ column indicates the targeted GRi% expressed in expected Σ TU: 0.5 TU = 25%; 1 TU = 50%; 1.5 TU = 75%. Observed TU_{50:50} describing biologically significant interactions (TU < 0.5 or TU > 2) are in **bold**.

	Σ TU	isoproturon + diuron				isoproturon + spiroxamine				isoproturon + metazachlor			
		Growth rate inhibition %			TU _{50:50}	Growth rate inhibition %			TU _{50:50}	Growth rate inhibition %			TU _{50:50}
		isoprotu ron	diur on	mixtu re		isoprotu ron	spiroxa mine	mixtu re		isoprotu ron	metazac hlor	mixtu re	
<i>T. lutea</i>	0.5	36.3 \pm 2.23	27.0 \pm 2.94	29.1 \pm 1.17	1.01 \pm 0.11	35.7 \pm 4.06	6.93 \pm 1.26	20.3 \pm 6.50	1.65 \pm 0.36				
	1	49.9 \pm 1.74	52.6 \pm 7.30	51.2 \pm 2.34		65.9 \pm 1.88	37.5 \pm 1.33	34.5 \pm 6.35					
	1.5	67.8 \pm 0.20	64.8 \pm 2.39	68.9 \pm 1.40		77.5 \pm 5.83	66.2 \pm 11.3	53.1 \pm 9.40					
<i>S. marinoi</i>	0.5	36.0 \pm 1.67	23.5 \pm 0.76	37.3 \pm 0.80	0.88 \pm 0.06	23.8 \pm 0.86	5.71 \pm 2.01	9.69 \pm 1.99	3.10 \pm 0.71	41.8 \pm 1.07	43.2 \pm 0.77	69.2 \pm 0.74	0.26 \pm 0.06
	1	69.1 \pm 0.35	58.6 \pm 1.40	67.8 \pm 1.99		58.9 \pm 0.31	84.4 \pm 1.44	18.9 \pm 1.93		74.2 \pm 0.27	52.5 \pm 1.06	80.7 \pm 1.00	
	1.5	77.4 \pm 0.22	73.7 \pm 0.17	78.3 \pm 1.19		71.3 \pm 1.06	100	32.3 \pm 0.80		83.1 \pm 0.98	54.4 \pm 0.83	84.3 \pm 0.24	